Landsat-based Irrigation Dataset (LANID): 30-m resolution maps of irrigation distribution, frequency, and change for the U.S., 1997-2017

Yanhua Xie[1,2], Holly K. Gibbs[1,2,3], Tyler J. Lark[1,2]

[1]Nelson Institute Center for Sustainability and the Global Environment (SAGE), University of Wisconsin-Madison, Madison, 53726, USA
[2]DOE Great Lakes Bioenergy Research Center, University of Wisconsin-Madison, Madison, 53726, USA
[3]Department of Geography, University of Wisconsin-Madison, Madison, 53706, USA

Correspondence to: Yanhua Xie (xie78@wisc.edu)

Abstract. Data on irrigation patterns and trends at field-level detail across broad extents is vital for assessing and managing limited water resources. Until recently, there has been a scarcity of comprehensive, consistent, and frequent irrigation maps for the U.S. Here we present the new Landsat-based Irrigation Dataset (LANID), which is comprised of 30-m resolution annual irrigation maps covering the conterminous U.S. (CONUS) for the period of 1997 – 2017. The main dataset identifies the annual extent of irrigated croplands, pastureland, and hay for each year in the study period. Derivative maps include layers on maximum irrigated extent, irrigation frequency and trends, and identification of formerly irrigated areas and intermittently irrigated lands. Temporal analysis reveals that 38.5 million hectares of croplands and pasture/hay have been irrigated, among which the yearly active area ranged from ~22.6 to 24.7 million hectares. The LANID products provide several improvements over other irrigation data including field-level details on irrigation change and frequency, an annual time step, and a collection of ~10,000 visually interpreted ground reference locations for the eastern U.S. where such data has been lacking. Our maps demonstrated overall accuracy above 90 % across all years and regions, including in the more humid and challenging-to-map eastern U.S., marking a significant advancement over other products, whose accuracies ranged from 50 to 80 %. In terms of change detection, our maps yield per-pixel transition accuracy of 81 % and show good agreement with U.S. Department of Agriculture reports at both county and state levels. The described annual maps, derivative layers, and ground reference data provide users with unique opportunities to study local to nationwide trends, driving forces, and consequences of irrigation and encourage the further development and assessment of new approaches for improved mapping of irrigation especially in challenging areas like the eastern U.S. The annual LANID maps, derivative products, and ground reference data are available through https://doi.org/10.5281/zenodo.5548555 (Xie and Lark, 2021a).

1 Introduction

Irrigated agriculture is vital to global food security. Irrigation helps stabilize farm production by enhancing land productivity that would otherwise be lower due to water limitations to plant growth. In the U.S., approximately 14.6 percent of the total cropland is irrigated (USDA-NASS, 2019). Despite this relatively small proportion, irrigated agriculture plays a significantly

disproportionate role in agriculture, accounting for major proportions of the economic value and environmental impacts; irrigated farms account for 54 percent of the total value of crop sales (USDA-NASS, 2021). However, agricultural irrigation uses over 40 percent of total freshwater withdrawals and 80 to 90 percent of consumptive water use in the U.S. (Dieter et al., 2018; USDA, 2019). As a result, improved management and understanding of irrigation use and trends offers a key leverage point to improve the sustainability of U.S. agriculture.

Knowledge of the spatial and temporal patterns of irrigation is a crucial first step to improve this understanding and management, and to help policymakers make decisions to support sustainable water use for crop production. However, the spatiotemporal patterns of irrigation and their impacts are not well understood, even for data-rich countries like the U.S. This lack of data and quality hampers a much larger body of research and applications, such as the modelling of land surface characteristics, climate and weather, and the growth of crops and other vegetation. For those applications that do incorporate irrigation modules, they are typically based on infrequently updated coarse-resolution global maps that cannot represent the precise locations of irrigated fields (Zaussinger et al., 2019; Ozdogan et al., 2010). As such, there is significant need for field-relevant resolution maps of irrigated agricultural land and its temporal changes. The value of such detailed irrigation information is further magnified as society formulates strategies towards sustainable use of limited water resources from local to global scales under the context of increasing food and fuel demands, climate change and extremes, and population growth (Lark et al., 2015; Rosegrant et al., 2009; Seto et al., 2012; Seager et al., 2012; Mcdonald et al., 2011).

Despite the growing importance of field-level irrigation information to a wide array of research questions and applications, currently available irrigation maps covering the entire or part of the Conterminous United States (CONUS) suffer from limitations related to spatial resolution, update frequency, geographical coverage, and mapping accuracy (Table 1). For example, the spatial resolution of all nationwide maps (except for LANID-US 2012) ranges from 250-m to kilometers, which is problematic for many local applications that require accurate field characterization (Wardlow and Callahan, 2014; Deines et al., 2017; Ozdogan and Gutman, 2008; Xie et al., 2019b; Brown and Pervez, 2014). Just as importantly, all these nationwide irrigation maps are infrequently updated and mapped at either a single date or at intervals of five years to decades (e.g., Shrestha et al. (2021), Brown and Pervez (2014) and Ozdogan and Gutman (2008)). Due to annual crop rotations, fallow practices, and climate variation, however, irrigation use and decision making are extremely dynamic. Accordingly, more timely information is needed to understand changes in irrigation and the associated impacts including water use and availability.

The recent years have witnessed an unprecedented development of land use/cover mapping owing to the increasing availability of high- to moderate-resolution remote sensing data and improvement of computing capacity (e.g., emergence of cloud computing platforms). While annual continental to global products of some land use/cover types have been created in a near operational manner (e.g., forest, water, and urban) (Hansen et al., 2013; Pekel et al., 2016; Gong et al., 2020), frequent fine-scale irrigation mapping remains challenging due to the cryptic nature of the irrigation signal and the lack of ground reference data needed to train and validate machine learning and other classifiers. The data gaps are particularly problematic in the midwestern and eastern U.S., where more abundant water resources have led to less concern and monitoring of irrigated land use.

Table 1. Currently available irrigation maps covering part to the entire CONUS. The boldfaced maps are compared with LANID in the Results section. (RF: random forest; RS: remote sensing)

Products	Spatial coverage	Resolution	Update frequency	Methods/datasets	Citations
Global Irrigated Area Map (GIAM)	Global	10 km rescaled to 1 km	Single map, 2000	Spectral matching/RS data	Thenkabail et al. (2009)
Global Map of Irrigation Areas (GMIA)	Global	10 km	5-year, 1995, 2000, and 2005	Spatial allocation/sub-nation statistics & maps	Siebert et al. (2005); Siebert et al. (2013)
Synthesized map of global irrigated area	Global	1 km	Single map, covering 1999-2012	Decision tree/RS, GMIA, & land cover maps	Meier et al. (2018)
Global Food-Support Analysis Data (GFSAD)	Global	1 km	Single map, 2010	Spectral matching/RS time series	Teluguntla et al. (2015)
Global Land Cover Map (GlobCover)	Global	300 m	Single map, 2009	Automatic classification/ RS time series	Esa (2015)
Global Land Cover Characteristics (GLCC)	Global	1 km	Single map, 1992	Hybrid compositing techniques/RS data	Loveland et al. (2000)
Global Rainfed, Irrigated and Paddy Croplands (GRIPC)	Global	500 m	Single map, 2005	Decision tree/RS, climate, & ag. inventory data	Salmon et al. (2015)
MODIS-based Irrigated Agriculture Dataset (MIrAD)	CONUS	250 m	5-year interval, 2002-2017	Thresholding/ag. Census & RS data	Pervez and Brown (2010)
MODIS-based Irrigation Fraction (MIF)	CONUS	500 m	Single map, 2001	Decision tree/RS time series	Ozdogan and Gutman (2008)
USDA-NASS Irrigation Statistics	U.S.	County-level	5-year interval, 1997-2017	Surveys	https://www.nass.usda.gov/AgCensus/index.php
USGS-verified irrigated lands	Western U.S.	Field	Vary across states, 2002-2017	Visual interpretation/RS & cropland inventory data	Brandt et al. (2021)
Landsat-based Irrigation Dataset 2012 (LANID 2012)	CONUS	30-m	Single map, circa 2012	RF/RS, climate, & envi data	Xie et al. (2019b)
Annual Irrigation Maps – High Plain Aquifer (AIM-HPA)	High Plains Aquifer	30-m	Annual, 1984-2017	RF/RS, climate, & envi data	Deines et al. (2019)
IrrMapper	Western CONUS	30-m	Annual, 1986-2018	RF/RS, climate, & envi data	Ketchum et al. (2020)

This paper presents the newly created annual 30-m resolution irrigation maps and their comparisons with existing products. The maps (named LANID – Landsat-based Irrigation Dataset) cover CONUS for the years between 1997 and 2017, which were built upon a past effort of irrigation mapping for the year 2012 (Xie et al., 2019b), with key improvements in training sample generation, classification design, and accuracy assessment (Xie and Lark, 2021b). The maps presented here also include a newly mapped component – irrigated pasture and hay – that was not explicitly included in the preliminary version presented in Xie and Lark (2021b). In addition to the LANID maps, we present the collected ground truth data, which is particularly important for irrigation mapping efforts that require such a dataset to train or validate machine learning algorithms, especially

where it has not been available in the humid eastern U.S. Additional products include maps of irrigation frequency, maximum extent, irrigation trends, formerly and intermittent irrigated areas. In the following sections, we briefly review the methods used to generate these data and then present our maps and their comparisons with existing products that cover the entire U.S.

2 Methods

Our new LANID product contains 21 annual maps that characterize irrigation status of croplands, pasture, and hay across CONUS for the years from 1997 to 2017. We first created annual maps of irrigated croplands (i.e., LANID_V1) using a supervised decision tree classification based on a novel training sample generation method and satellite-derived and environmental variables (see details in Xie and Lark (2021b)). Because LANID_V1 does not explicitly include irrigated pasture and hay, which is an important component of total irrigation particularly in the western U.S., we addressed this limitation by applying the same machine learning method but using different mask layers and areal reference for training sample generation and classification (Fig. 1). The maximum extent of pasture and hay for the west was derived from the USGS National Land Cover Database (NLCD) and USDA Cropland Data Layer (CDL), identifying pixels that had been classified as pasture/hay in NLCD or non-alfalfa hay in CDL within any year between 1992 and 2017. To reduce competition between this pasture and hay mask and the one used for irrigated cropland mapping, we removed those pixels that had been classified as irrigated cropland in LANID_V1. The county-level areal reference of irrigated pasture and hay was calculated as the deficit of LANID_V1-based irrigated cropland area compared to USDA NASS reported area, which includes all types of irrigated agriculture.

A key element of the LANID methodology is a novel way to generate training samples covering the entire country. To account for climate difference and mapping complexity, CONUS was divided into western and eastern states based on a climatic transition near the 100th meridian and training data were created corresponding to each region (Fig. 2). We used an automated method to generate training samples for the western states. For the years when USDA-NASS county-level irrigation statistics are available (i.e., 1997, 2002, 2007, 2012, and 2017), we adopted the thresholding method proposed by Xie et al. (2019b) to automate training sample generation, which assumed that irrigated lands appear greener than those that are rainfed. For non-census years, optimal thresholds were estimated based on relationships of crop greenness between non-census and census years. The calibrated and estimated thresholds were used to segment yearly maximum Landsat-based greenness index (GI) and enhanced vegetation index (EVI) to derive two intermediate irrigation maps per year, which were overlaid to identify consistent classification as potential training samples. As a result, the generated potential training samples were evenly distributed across the western CONUS on a yearly basis.

For the relatively humid eastern states, we visually collected samples through interpretation of multi-temporal very high-resolution images, street views, and time-series Landsat data on Google Earth and Google Earth Engine, based on the appearance of irrigation infrastructure such as wells, pipes, center pivot towers, and circular field patterns. Detailed methods of sample generation are described in Xie and Lark (2021b).

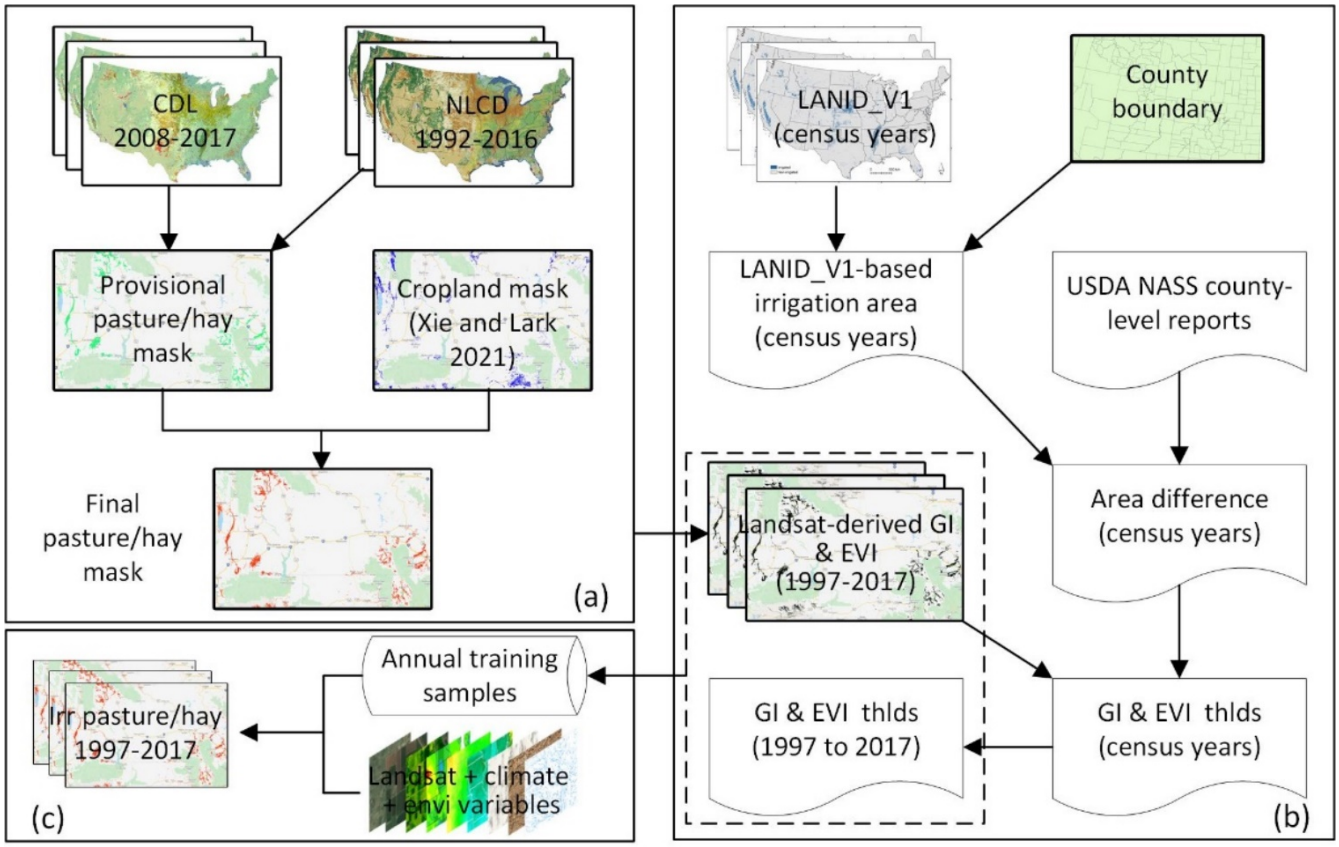

Figure 1: Flowchart of mapping irrigated pasture and hay in western U.S. (a) generating the maximum extent of pasture/hay; (b) creating training samples, and (c) classification. Cropland mask refers to the maximum extent of non-pasture/hay cultivated land created in Xie and Lark (2021).

The predictors generally consist of two categories – satellite data and environmental variables (Xie and Lark, 2021b). The primary satellite-derived variables were calculated from all available Landsat images within each year, including yearly maximum, median, and range composites of GI, EVI, and normalized difference water index (NDWI). Annual and late-season (May 1 to October 15) sum of MODIS-derived indices (i.e., EVI and land surface temperature) were also used as additional variables. Environmental variables included annual and late-season sum of irrigation-relevant climate variables (i.e., precipitation, temperature, partial pressure of water vapor), elevation and slope, soil water content, and distance to major rivers (Deines et al., 2017; Deines et al., 2019; Xu et al., 2019; Xie et al., 2019b). Altogether, there were 32 input features (25 for the years 1997-2000 when MODIS products were not available).

Classification was implemented on Google Earth Engine, a cloud-computing platform that enables rapid accessing and processing of vast numbers of satellite images, climate data, and geophysical products (Gorelick et al. 2017). The classification was conducted annually per county using the widely used random forest classifier (Breiman 2001). The county-level classifications were mosaiced to create an initial time-series nationwide irrigation map, followed by logic and spatial filtering to remove possible false classification (see details in Xie and Lark (2021b)).

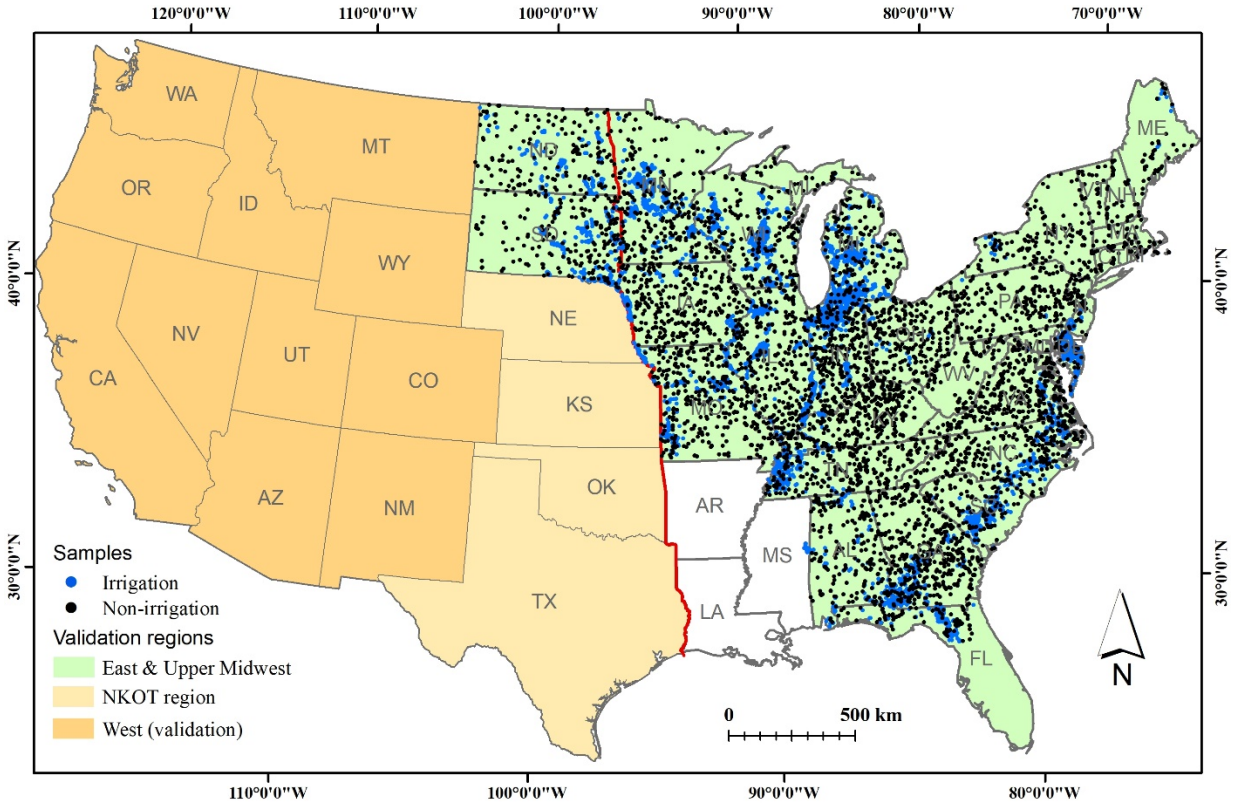

Figure 2: Map evaluation and comparison design and the distribution of test sample locations across the eastern CONUS. The NKOT region refers to Nebraska, Kansas, Oklahoma, and Texas, which covers the majority of the High Plains Aquifer. The red solid line represents the West-East division for classification only.

3 Map evaluation and comparison design

Comprehensive assessment of nationwide irrigation maps is not possible without adequate ground truth data, especially for the eastern U.S. Therefore, accuracy of many published irrigation maps covering CONUS have been poorly evaluated. We compared our LANID maps to existing nationwide irrigation-specific maps, including two binary maps (i.e., MIrAD and GIAM) and two maps of irrigation fraction (i.e., MIF and GMIA areal percentage equipped for irrigation) (Table 1). Other global maps that include irrigation-related classes, such as Global Land Cover Map and GFSAD, are not shown because they are not irrigation-specific and substantially under-represent irrigation extent across CONUS. In addition to coarser resolution nationwide maps, we also compared our maps with recently available 30-m resolution maps for the High Plain Aquifers and the eleven western states, i.e., AIM-HPA and IrrMapper, respectively.

Map evaluation and comparison were conducted by using test samples from two sources that cover the majority area of CONUS – a published reference dataset from Ketchum et al. (2020) and an additional independent dataset that we collected for this study. The test samples from Ketchum et al. (2020) were collected through visual interpretation of field parcels based on irrigation clues from VHR images and crop greenness. The dataset has approximately 100,000 sample points, covering 11

western states (Fig. 2) for the whole study period of 1997-2017. Our independently collected validation samples (approximately 10,000 locations) covered the remaining areas except for Arkansas, Louisiana, and Mississippi. Lastly, we evaluated LANID's capability to detect irrigation change from pixel to state scales.

4 Results

4.1 Irrigation samples across the eastern U.S.

To validate our maps, we collected approximately 10,000 irrigation and rainfed samples for the east (~5,000 for each category) (Fig. 2). Each irrigation sample records a center pivot location and the presence of irrigation infrastructure during 1997-2017 (Fig. 3). In addition, we measured the radius of each center pivot irrigation system, i.e., the distance from its center to its field boundary. Note that the length of corner arms (designed for corner irrigation) was not measured (e.g., Field #1 in Fig. 3). Stable non-irrigation samples record the locations with clear evidence of no irrigation infrastructure during the entire mapping period. The average pivot radius for all samples collected in the Eastern CONUS was 330 meters, but distributed bimodally around approximately 200 and 400 meters, which correspond respectively to broader rectangular circumscribed crop fields of 40 and 160 acres.

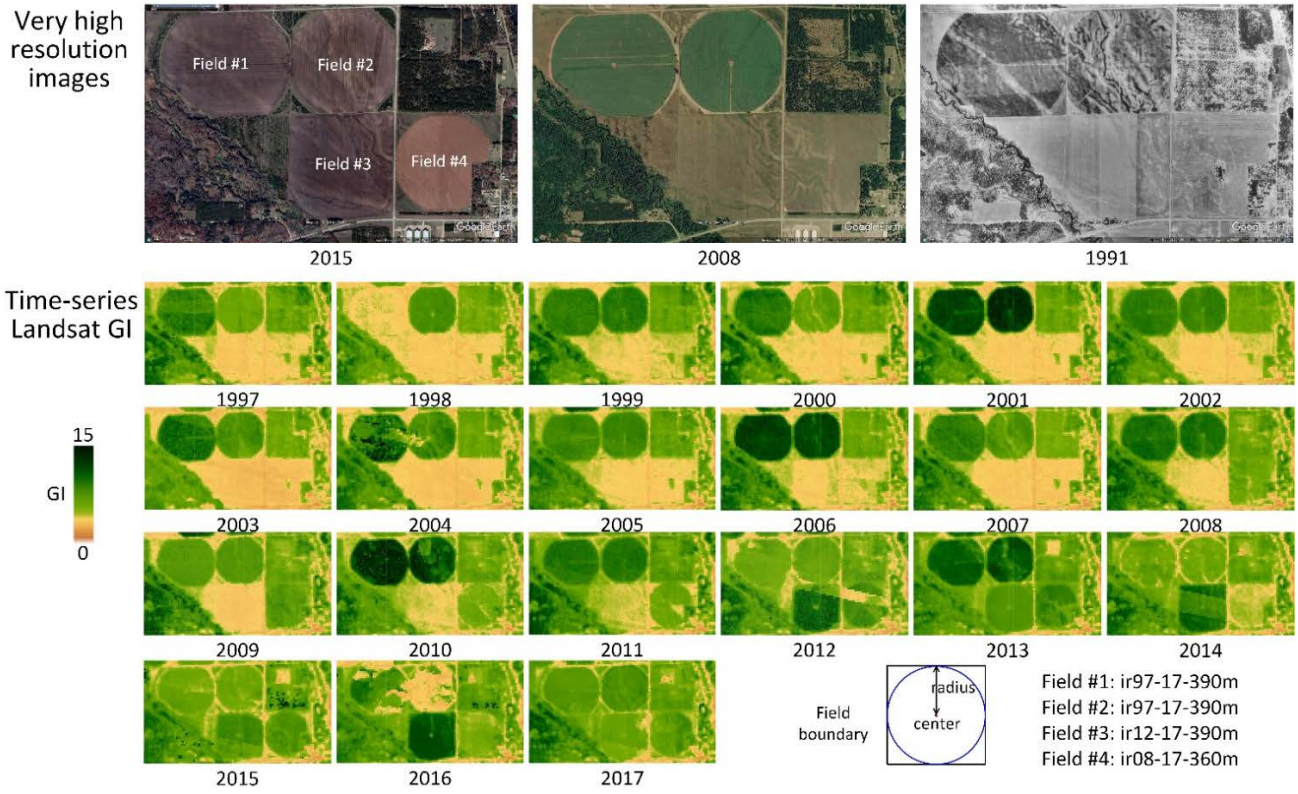

Figure 3: Demonstration of center-pivot irrigation field collection using time-series very high-resolution (© Google Earth Pro 2021) and Landsat images. GI: greenness index.

4.2 Irrigation trends and changes

Our LANID reveals a steady increase of irrigated area throughout CONUS, although there are some years with exceptional, lower values – for example, 2012 and 2002, years in which there were significant drought (Fig. 4) (Otkin et al., 2018). Overall, irrigation area has increased by around 1.5 million hectares (Mha) during the period, from ~23 Mha before 2000 to ~24.5 Mha in 2016 with an average annual increase of ~80,000 ha. Consistent with earlier findings, the Central Valley of California, the High Plains portion of Texas, South-Central Florida, as well as select western states (e.g., Utah, Colorado, Idaho, and Wyoming) experienced substantial irrigation loss during the period (per-state plots in Fig. 4). In contrast, irrigation increased in states across the Midwest (including Nebraska, North Dakota, and South Dakota), the Mississippi Alluvial Plain, and the East Coast. The largest gains occurred in Nebraska, Missouri, Michigan, Illinois, Arkansas, Mississippi, and Indiana, where irrigated area grew by over 100,000 ha per state.

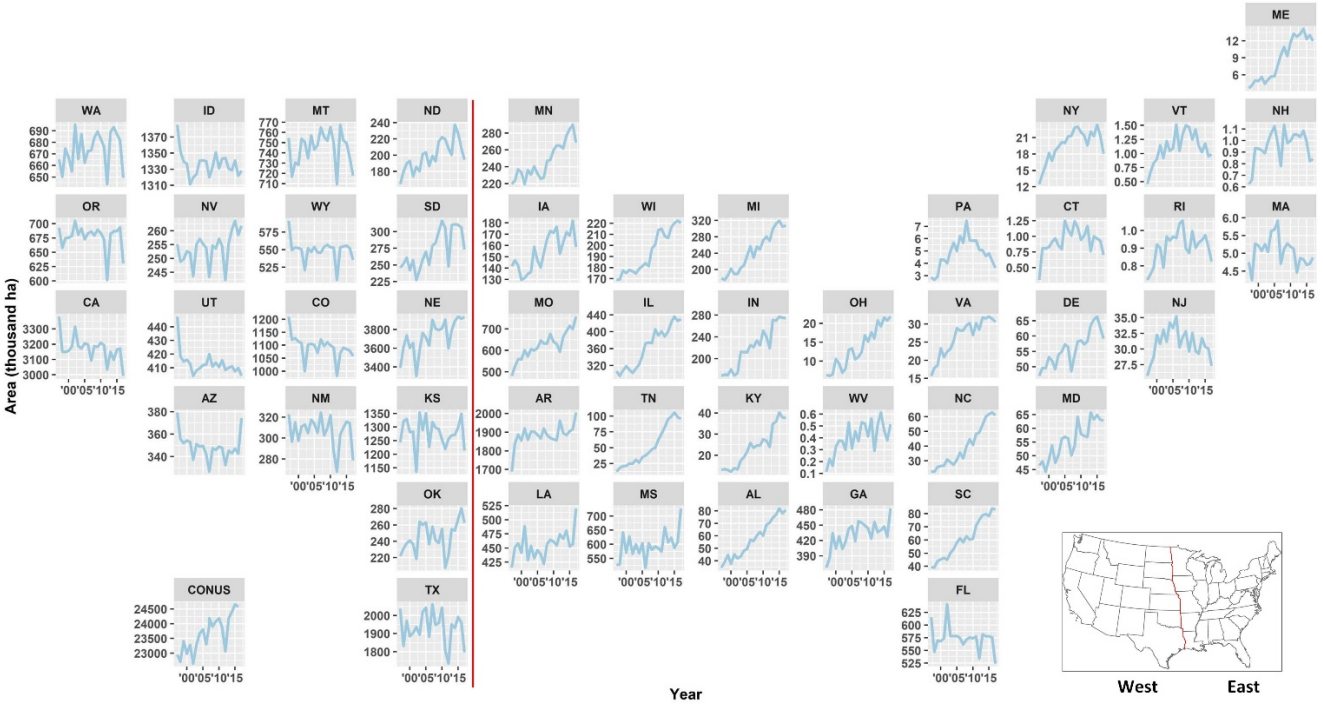

Figure 4: LANID-derived annual irrigation area by state, 1997-2017. The red line shows the East-West division in this study based on a climatic transition near the 100th meridian. Annual irrigation area per state is provided in Table A1.

Our LANID-derived irrigation changes agree well with USDA-NASS Census-reported values (with R^2 from 0.81 to 0.96), indicating that LANID and the USDA-NASS data are consistent in their detection of irrigation change at both county and state scales. Relative to the NASS data, however, our LANID maps predict slightly greater irrigated extent at the national level and slightly fewer net changes at both state and county levels, especially for the eastern CONUS (Fig. 5).

Aggregating the annual LANID maps to a finer but still intermediate 6-km resolution can reveal more localized trends than state- or county-level data allow, while also accommodating for the field-level stochasticity and variations that often occur

within a single farm or shared water source (Fig. 6). Such a resolution is particularly helpful for identifying small pockets of change with countervailing trends that would otherwise be masked or undetected. For example, we found outlier locations of irrigation loss in the Mississippi Alluvial Plain and of irrigation gain in the central and southern High Plains Aquifer.

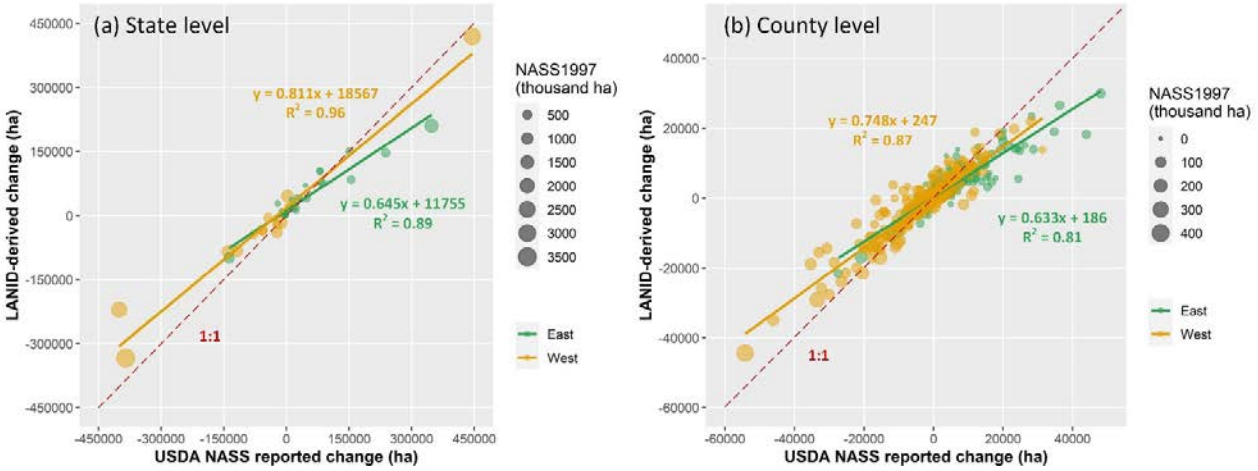

180 **Figure 5: LANID-derived irrigation changes vs. USDA-NASS reported area at the state (a) and county (b) scale. Irrigation change was calculated as the difference between mean area of years 2012 and 2017 and that of 1997 and 2002 (i.e., mean($irArea_{2012}$ + $irArea_{2017}$) – mean($irArea_{1997}$ + $irArea_{2002}$) where $irArea_{yr}$ refers to irrigation area of year *yr*). The USDA-NASS reported values of 1997 is shown to represent irrigation area at the starting point of the study period.**

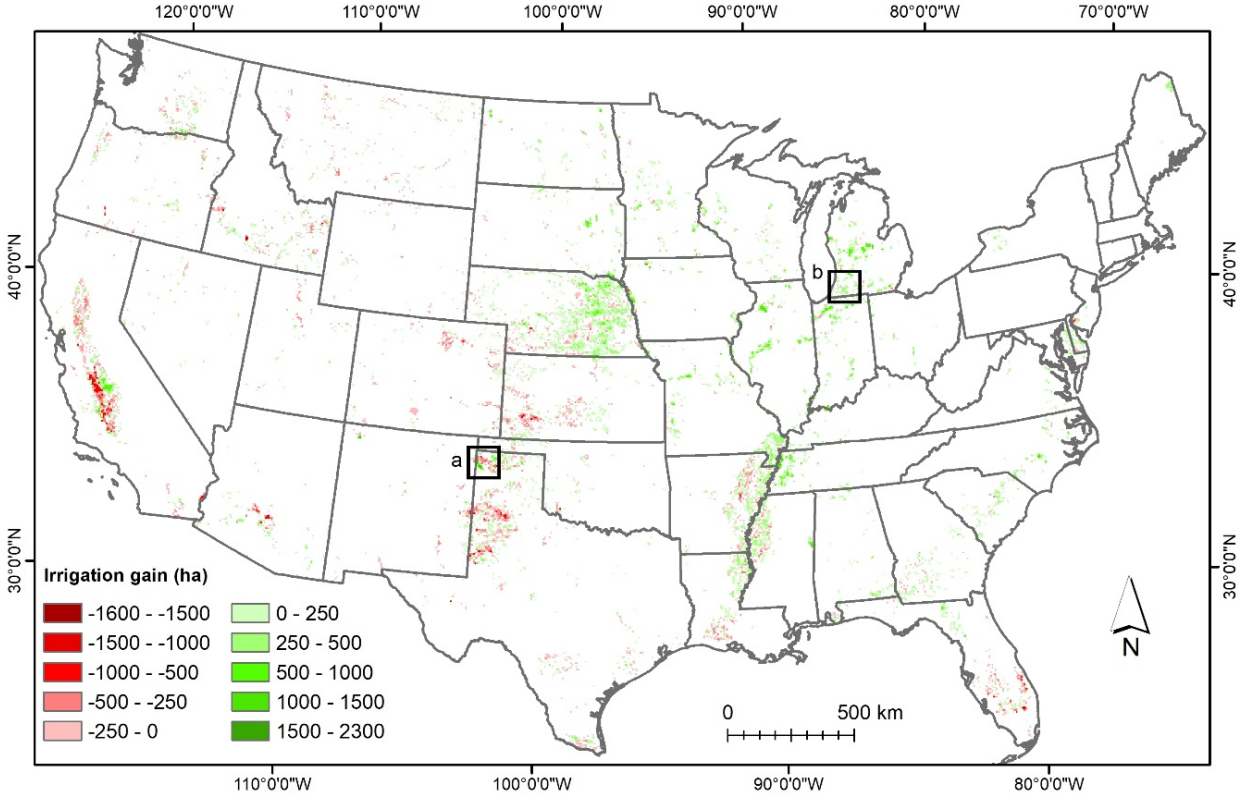

Figure 6: LANID-derived irrigation gain from 1998-2007 to 2008-2017 at the 6km×6km scale. Per-grid value is calculated as the difference between mean irrigation area of 1998-2007 and that of 2008-2017 (i.e., meanIrArea$_{2008-2017}$ - meanIrArea$_{1998-2007}$, where irArea is LANID-aggregated irrigation area within a 6km×6km grid). Grids with absolute change < 2.5 % of are shown as background.

Ultimately, when applied at the highest resolution, our LANID maps can be used to reliably characterize irrigation dynamics at sub-field to field level with overall accuracy and Kappa index of 81 % and 0.62, respectively (Table 2). For instance, sub-field to field level expansions, losses, and interannual variations of irrigation that are detectable from LANID can be clearly observed in north Texas (Fig. 7a). Although such a level of change detection in more humid areas is not as effective as more arid states due to a weaker contrast between irrigated and rainfed fields, LANID still provides a reasonable and accurate characterization of irrigation change through time there as well, as shown in the example in Michigan (Fig. 7b).

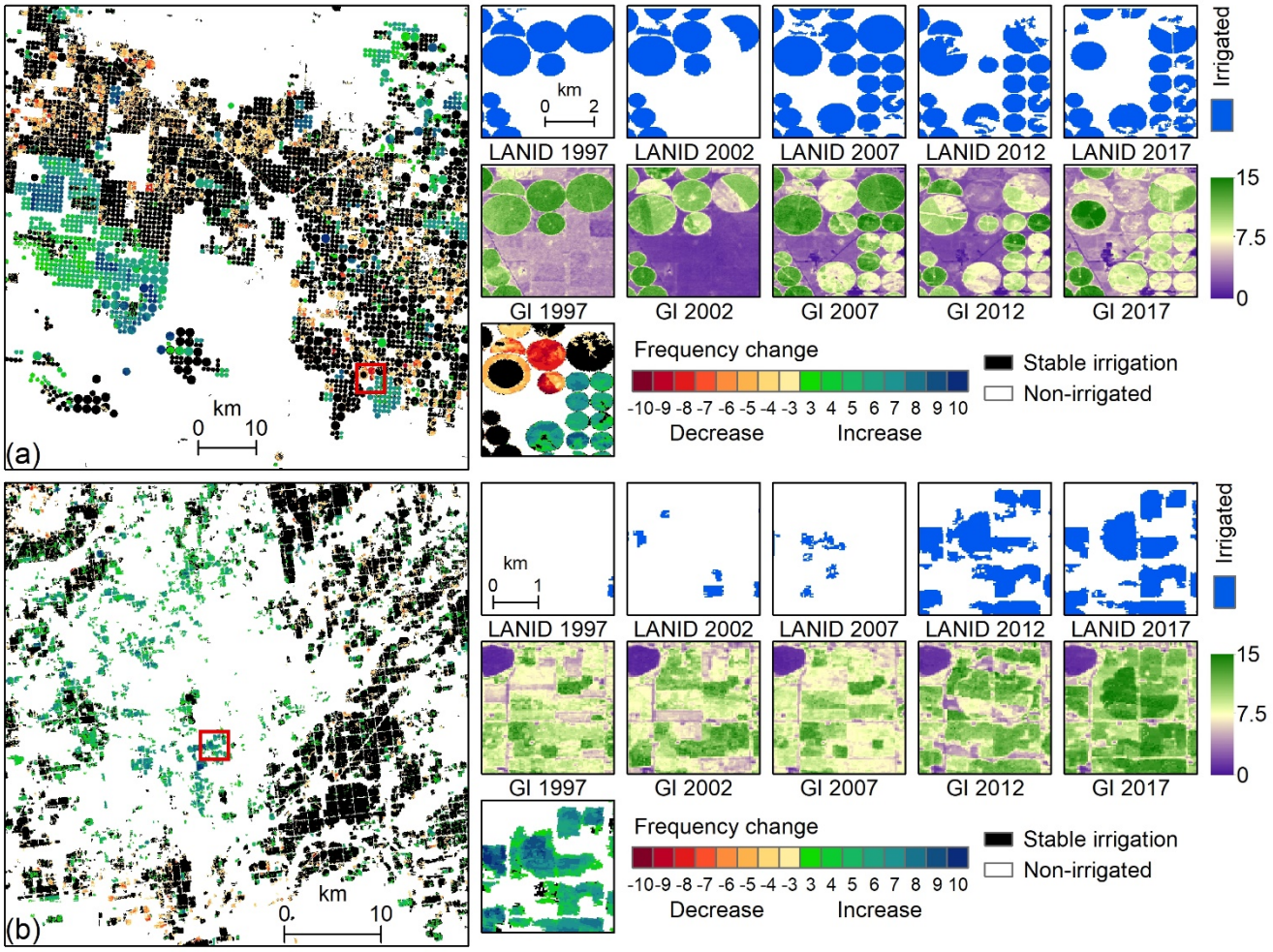

Figure 7: Demonstration of LANID-derived field-level irrigation frequency change for the northern Texas (a), and southwestern Michigan (b), respectively (highlighted in Fig. 6). Frequency change refers to the difference of number of years irrigated between 1998-2007 and that of between 2008-2017 (i.e., irFreq$_{2008-2017}$ - irFreq$_{1998-2007}$, where irFreq is the number of years irrigated).

Table 2. Accuracy of change detection using LANID maps. Change is defined as frequency difference between the two sub-periods (i.e., 1998-2007 and 2008-2017) greater than 3 and the stable class refers to the value smaller or equaling to 3. Note non-agriculture is excluded from the stable class.

		Reference		
		Stable	Change	User's accuracy
Classified	Stable	187	63	75 %
	Change	13	137	91 %
	Producer's accuracy	94 %	69 %	
	Overall accuracy: 81 %; Kappa: 0.62			

4.3 Irrigated pasture and hay

This study provides the first complete mapping and delineation of irrigated pasture and hay for the western U.S. (Fig. 8). In this region, forage and fodder crops provide valuable feed for livestock and irrigation is often necessary to cultivate certain species or attain viable yields. This contrasts with pasture and hay in the eastern states, where annual precipitation and soil moisture is typically sufficient for robust production of grass-based forage and fodder. Areas of irrigated pasture and hay have a pattern of land use distinct from that of irrigated croplands, as well as unique implications for water use and the environment.

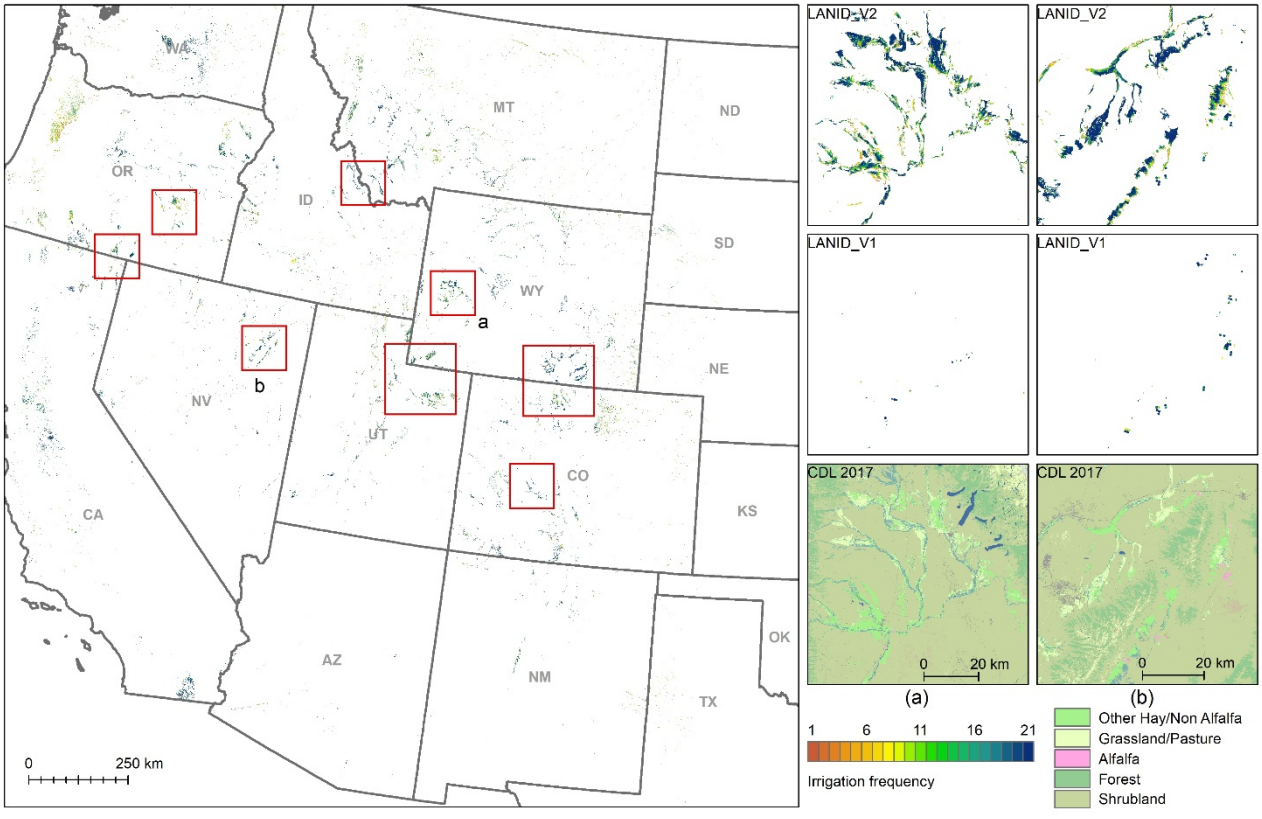

Figure 8: Distribution of irrigated pasture and hay derived from LANID_V2 (presented in this study) in the western CONUS. The overview display shows irrigation frequency (i.e., the number of years a pixel is irrigated during 1997-2017). The highlighted areas under red rectangle represent areas of intensively irrigated pasture and hay that were not completely mapped in LANID_V1. (a) and (b) are example local views for western Wyoming and northeastern Nevada, respectively.

Compared to the first version of LANID, which did not explicitly include irrigated pasture/hay, we found an average of 0.34 Mha more irrigated land (i.e., more irrigated pasture and hay included in LANID_V2 compared to LANID_V1) for the years 2013 to 2017, and a similarly larger amount (0.36 Mha) since the start of the study period. This increase in irrigated extent is lower than that of the USDA Census of Agriculture's estimate of 1 Mha of irrigated pasture – the only other spatial (but coarse) estimate of such irrigated land use (Sanderson et al., 2012). The difference between our annual estimates and that of the Census data likely reflects the fact that a large portion of irrigated pasture and hay (especially alfalfa) had already been mapped in the first version of LANID. To confirm this, we further calculated a direct estimate of only irrigated pasture/hay as all irrigated pixels classified as pasture or hay in the NLCD or CDL and estimated an average area of 1.39 Mha across the years 2008, 2011, 2013, and 2016. This estimate is 0.39 Mha higher than the 1 Mha reported by the Agricultural Census but includes both pasture and hay, whereas the Census estimate is for pasture only.

4.4 Maximum extent, frequency, and formerly and intermittent irrigated land

Across all types of irrigation – including cultivated cropland and pasture and hay – a total of 38.5 Mha of land were irrigated at least one time between 1997 and 2017, representing the maximum irrigated extent in the U.S. for our study period (Fig. 9a and Table 3). Of these areas, just 24.2 Mha (62.8 %) were irrigated in 2017, and this annual utilization percentage ranged from 58.8 to 64.0 % over the full study period. Across all pixels within the maximum irrigated extent, the mean annual irrigated frequency was 12.9 out of 21 years (Fig. 9b). The distribution of irrigated frequency suggests many areas consist of stable, persistent irrigation, but that there also exists a substantial amount of land with intermittent irrigation use. Those pixels with the very lowest irrigation frequency likely reflect locations where irrigation ceased very early in the study period or was first initiated very late in the study period, and/or areas of potential misclassification.

Looking at the subset of lands that are no longer irrigated, we found 4 Mha of formerly irrigated land (i.e., not irrigated anytime in the most recent 3 years, 2015-2017, but that were irrigated at least 3 times prior) (Table 3). This formerly irrigated land is primarily distributed across the western states (as showed in Fig. 6), and may reflect areas where insufficient water availability has limited the ongoing use, or where salination of soils, socioeconomic drivers, or other superseding factors have resulted in a cessation of irrigated agriculture. Of these formerly irrigated areas, 71.6 % remain in crop production under rainfed conditions, primarily planted to corn (13.2 %), soybeans (12.3 %), and spring/winter wheat (12.2 %) as of 2017. The remaining locations have either been abandoned from cultivated crop production altogether (26.3 %) or converted to urban use (2.1 %). Those areas for which an irrigated crop is no longer viable may represent an opportunity for farmers to transition to grassland-based agriculture (Deines et al., 2020), for example via the introduction of pasture for livestock grazing or the harvesting of biomass for use as forage or cellulosic bioenergy feedstock (Robertson et al., 2017). As climate change and decreasing freshwater availability continue to strain water resources, the total area of formerly irrigated lands is likely to increase, thereby

creating even further opportunity and greater need for alternative, drought resistant agricultural opportunities, such as those afforded by perennial feedstock production.

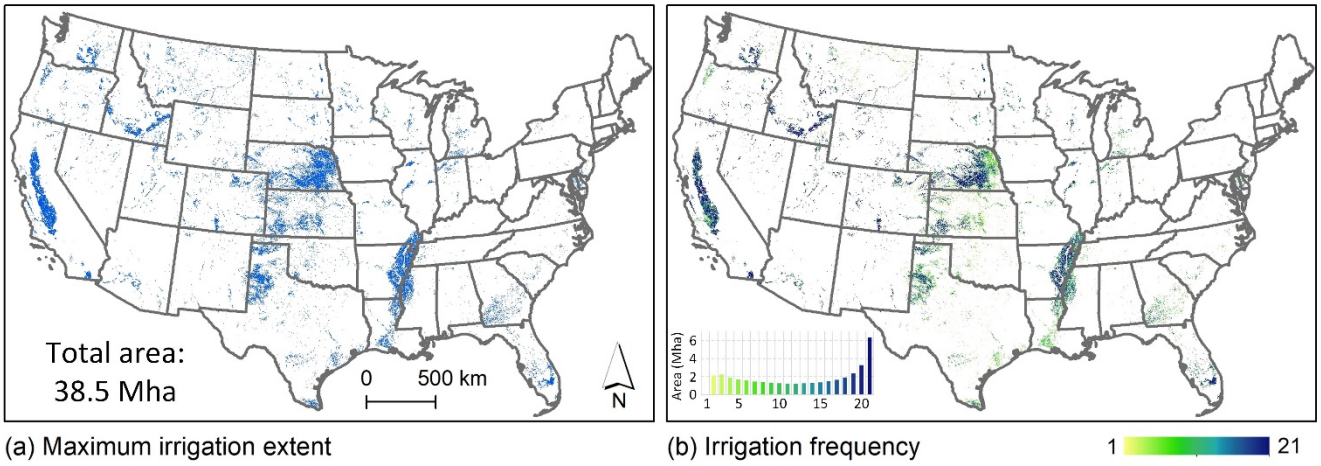

Figure 9: The maximum irrigation extent (lands that have been irrigated at least once) and irrigation frequency (the number of irrigated years) across CONUS for the period 1997-2017. The inset in (b) shows the area of each frequency value.

In addition to those locations where irrigation has ceased completely, we observed a substantial amount of land where irrigation remained active in the most recent years but where its use across time was discontinuous. For example, we found 25.5 Mha of land across CONUS that had been irrigated spanning the whole study period (i.e., irrigated at least once for both 1997-1999 and 2015-2017), where over half of that subset (i.e., 13.5 Mha) could be best described as intermittently irrigated (frequency ≤ 18) (Table 3). As opposed to those locations with continuous annual irrigation use or where irrigation has ceased altogether, these intermittently irrigated lands appear to remain in irrigated agriculture today yet rely on such irrigation use just 67 % (median value) of the time across the 21-year study period. While further investigation is needed to better characterize these areas of partial irrigation use over time, it may be possible that they represent locations where irrigation is only supplemental (e.g., used only in dry years or when needed), shared among a single water source but rotated among multiple nearby fields, or used only in years with sufficient water availability or water application rights and allocations. Similar to formerly irrigated lands, these locations of intermittent irrigation application may present areas of opportunity or economic need for alternative, rainfed agriculture in non-irrigated years. In such cases, drought tolerant annual crops like forage or energy sorghum could potentially provide economic opportunities for producers and limited further strain on local hydrology (Enciso et al., 2015; Mullet et al., 2014; Cui et al., 2018).

Table 3. Statistics of irrigation area (in million hectares) across CONUS for the period 1997-2017.

	Area	Definition
Average annual area	23.7	Mean annual irrigation area
Maximum area	38.5	Irrigated at least once
Formerly irrigated	4.0	Not irrigated anytime in 2015-2017, but irrigated at least 3 times prior

Long-term irrigation	Intermittently irrigated	13.5	Irrigated at least once for both 1997-1999 and 2015-2017, and irrigation frequency ≤ 18
	Continuously irrigated	12.0	Irrigated at least once for both 1997-1999 and 2015-2017, and irrigation frequency > 18

4.5 Comparisons with existing products

Figure 10 presents the nationwide view of a single year LANID as well as other irrigation-specific products. The 30-m LANID 2005 map was aggregated to 10-km resolution (Fig. 10b) for comparing with other coarser resolution maps. Across broad scales, all maps show similar irrigation hotspots of the High Plains Aquifer, the Central Valley Aquifer, the Mississippi Alluvial Plain, the Snake River Aquifer, and the East Coast. While it might be reasonable to conclude that all these coarse resolution maps can capture similar irrigation patterns at the national scale, regional views emphasize the details that are uniquely captured by LANID. For instance, LANID identifies fewer irrigated pixels at the eastern Columbia Plateau Aquifer than other maps, especially compared to MIF and GIAM (Fig. 11). In another example of the High Plains Aquifer, GIAM and MIF substantially overestimate irrigation extent in the western and central Kansas compared to both LANID and MIrAD (Fig. 12). Among all comparison products, MIrAD provides the most similarity of irrigation patterns as LANID in the arid to semi-arid West and Midwest.

In more humid areas like the upper Midwest, our LANID map captures patterns that are considerably misclassified by other maps (Fig. 13). For example, GIAM and MIF omit the majority of irrigated fields in the region; MIrAD shows a clear administrative boundary effect and near random distribution of irrigation within each county. At 10 km resolution, GMIA provides similar patterns as LANID but exaggerates the overall irrigation extent.

Locally, LANID shows a substantial improvement of spatial detail compared to other maps. For example, boundaries of center pivot and rectangular fields are clearly recognizable in LANID, while they are obscured even on the 250 m resolution MIrAD (insets (h) and (j) of Figs. 11 and 12). It is also evident that LANID shows comparable spatial details as other regional maps IrrMapper and AIM-HPA (inset (i) of Figs. 11 and 12) while still offering consistent and comprehensive coverage across the CONUS.

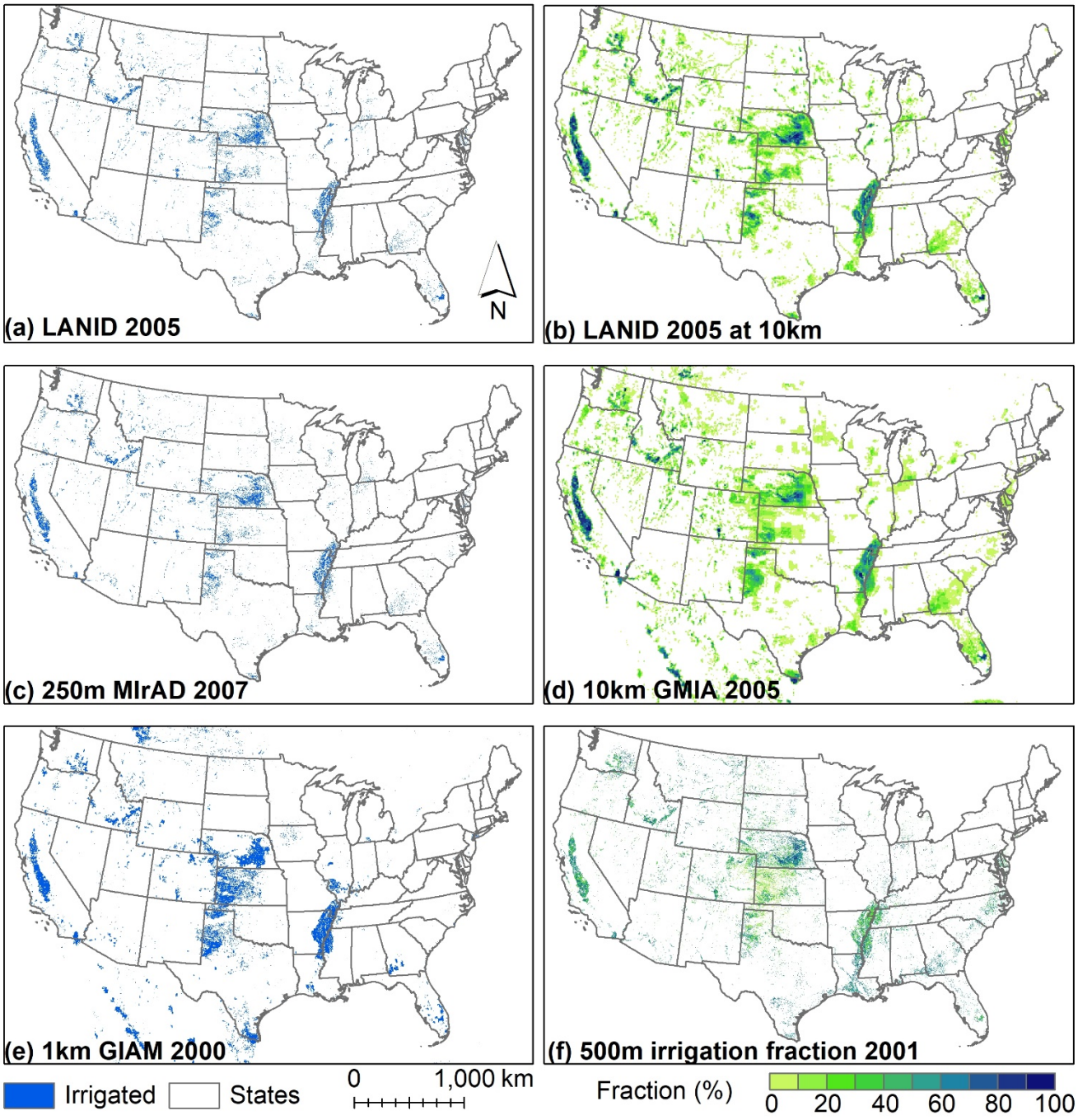

Figure 10: Nationwide views of different irrigation mapping products. LANID 2005 is aggregated to 1 km (a) and 10 km (d) resolution for comparison purpose. The LANID-derived irrigation frequency refers to the number of years a pixel is classified as "irrigated".

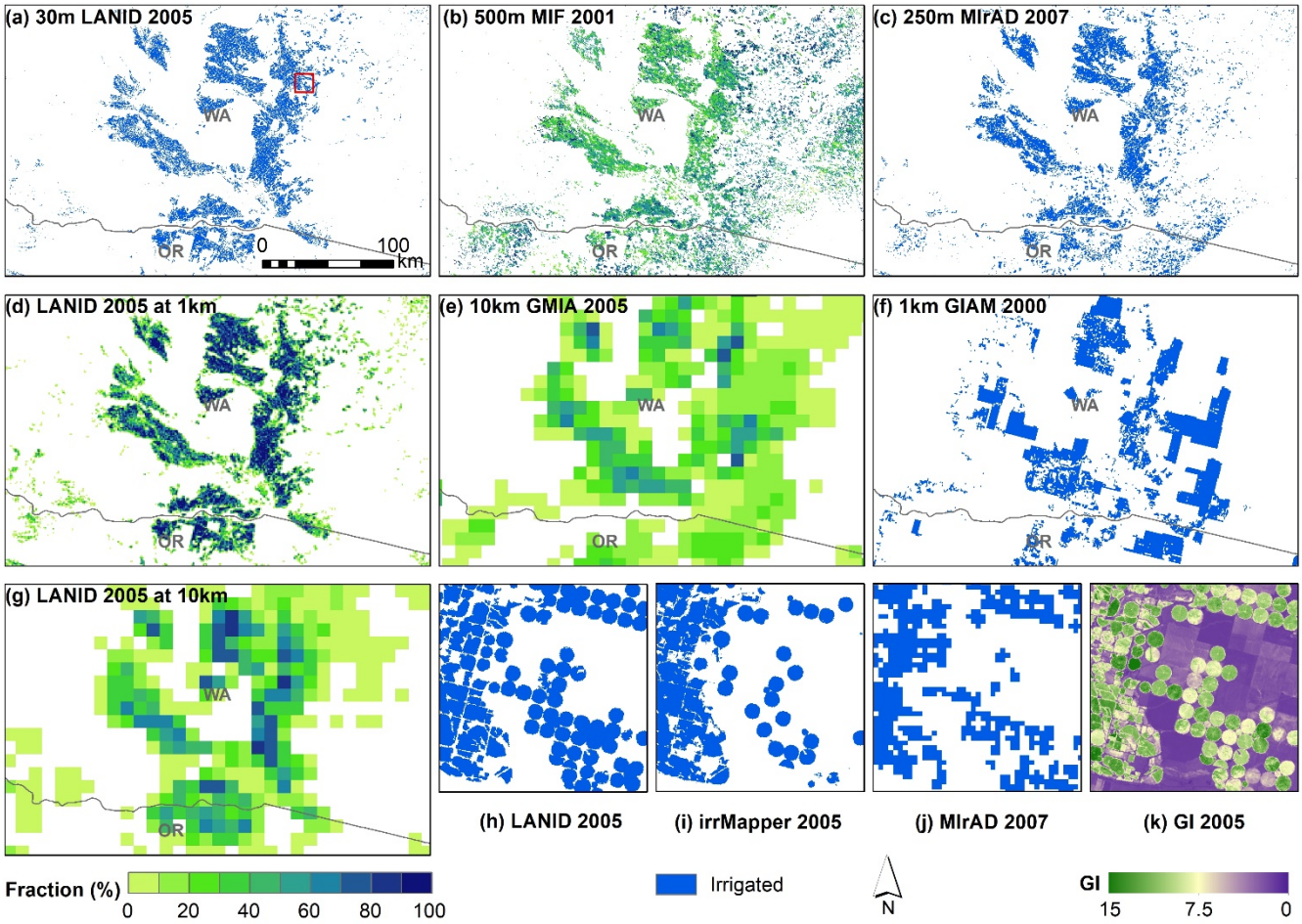

Figure 11: Product comparison at the Columbia Plateau Aquifer in northern Oregon and southern Washington. In addition to the original 30-m LANID (a), the map is aggregated to 1 km and 10 km resolution for displays (d) and (g). (h)-(i) show the location highlighted in (a) (red rectangle).

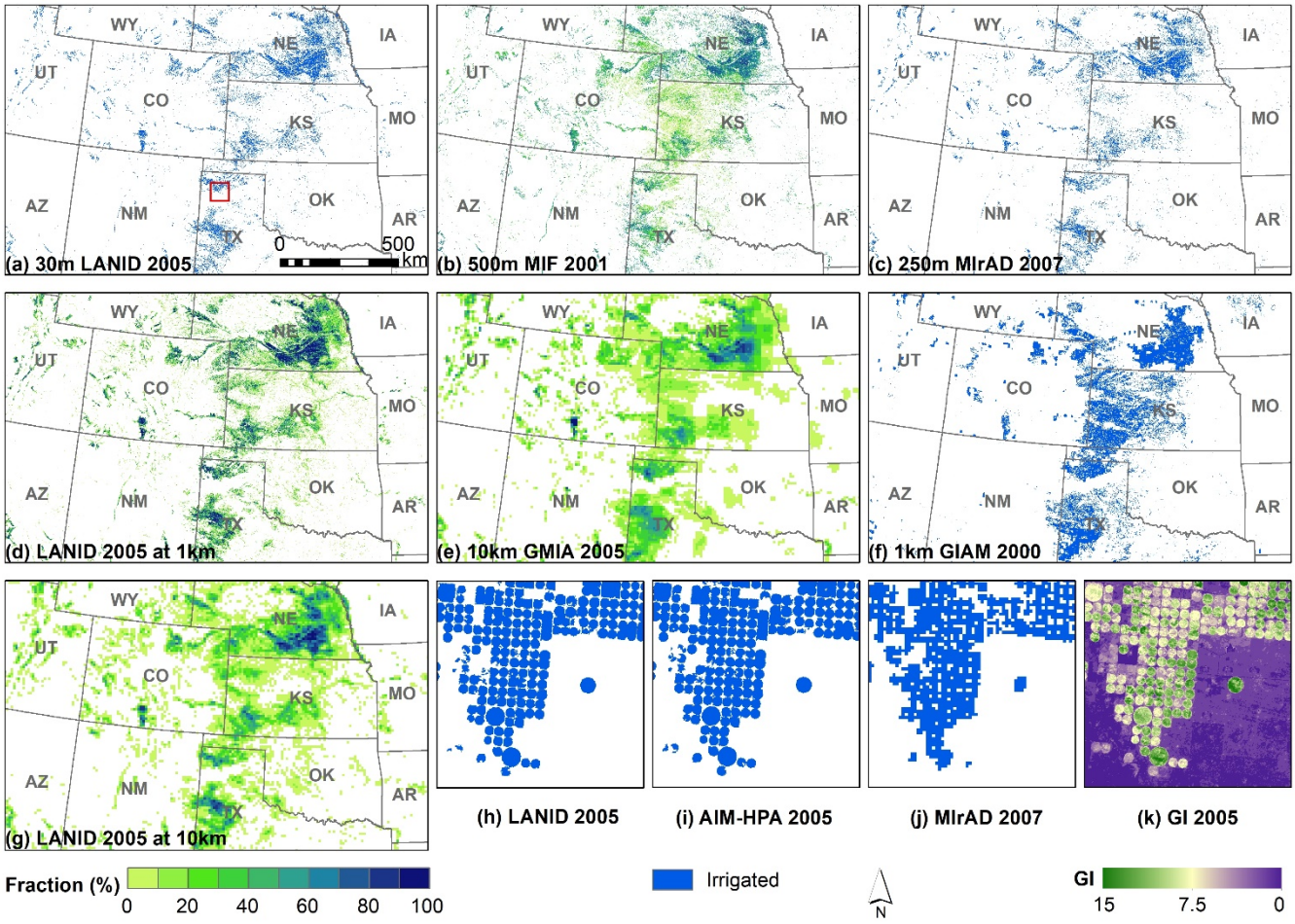

Figure 12: Product comparison at the High Plains Aquifer. In addition to the original 30-m LANID (a), the map is aggregated to 1 km and 10 km resolution for display (d) and (g). (h)-(i) show the location highlighted in (a) (red rectangle).

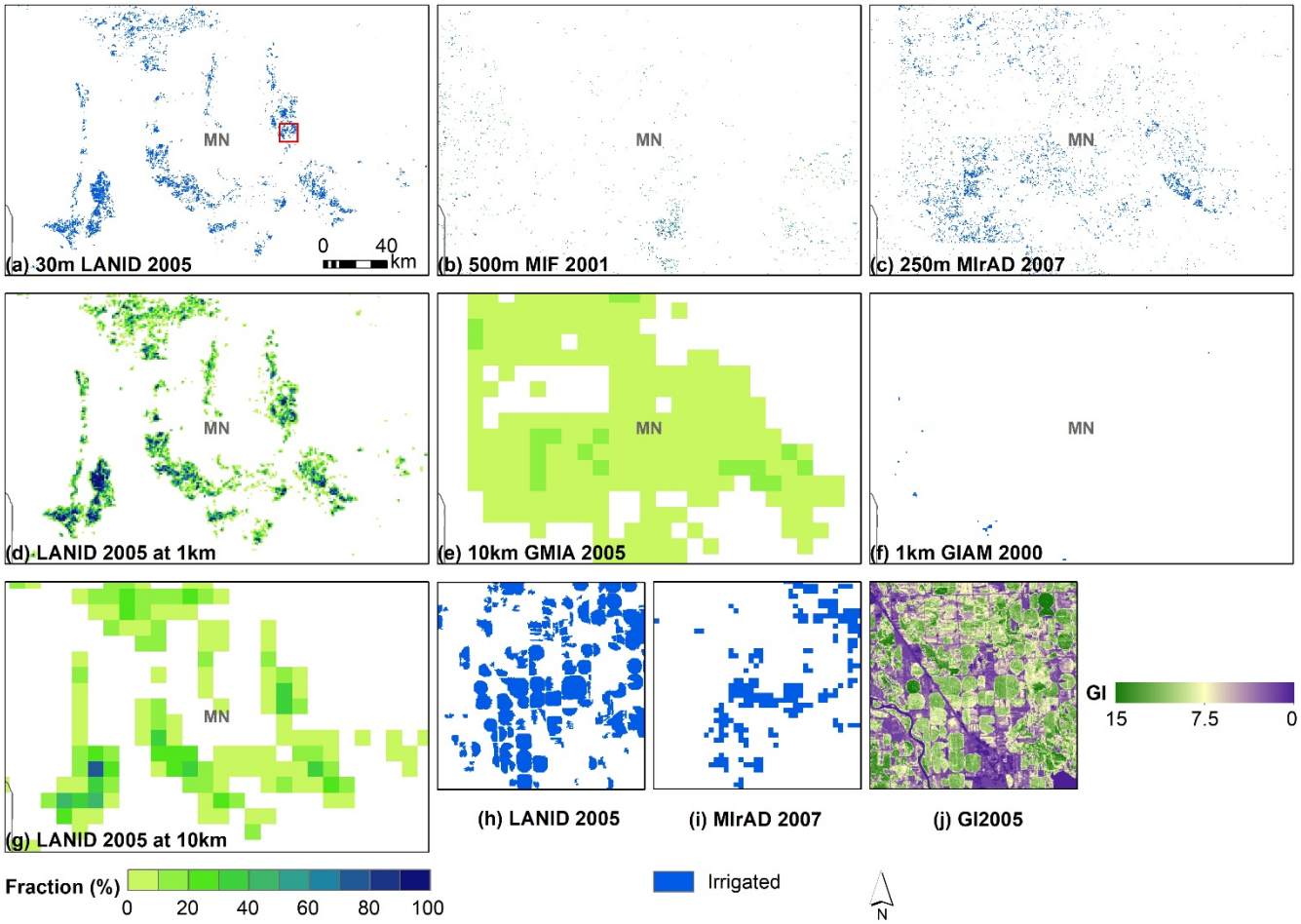

295 **Figure 13: Product comparison in central Minnesota. In addition to the original 30-m LANID (a), the map is aggregated to 1 km and 10 km resolution for display (d) and (g). (h)-(i) show the location highlighted in (a) (red rectangle).**

At the state level, our LANID estimates are consistent with USDA-NASS reported data (Fig. 14b), although the agreement is weaker than that of products like MIrAD and GMIA, which both rely directly and exclusively on census data as areal reference (not shown in the figure). In contrast, MIF underestimates irrigated area at the state level (Fig. 14c), whereas GIAM
300 substantially overestimates irrigation extent especially for the states with reported area greater than one million hectares (Fig. 14d).

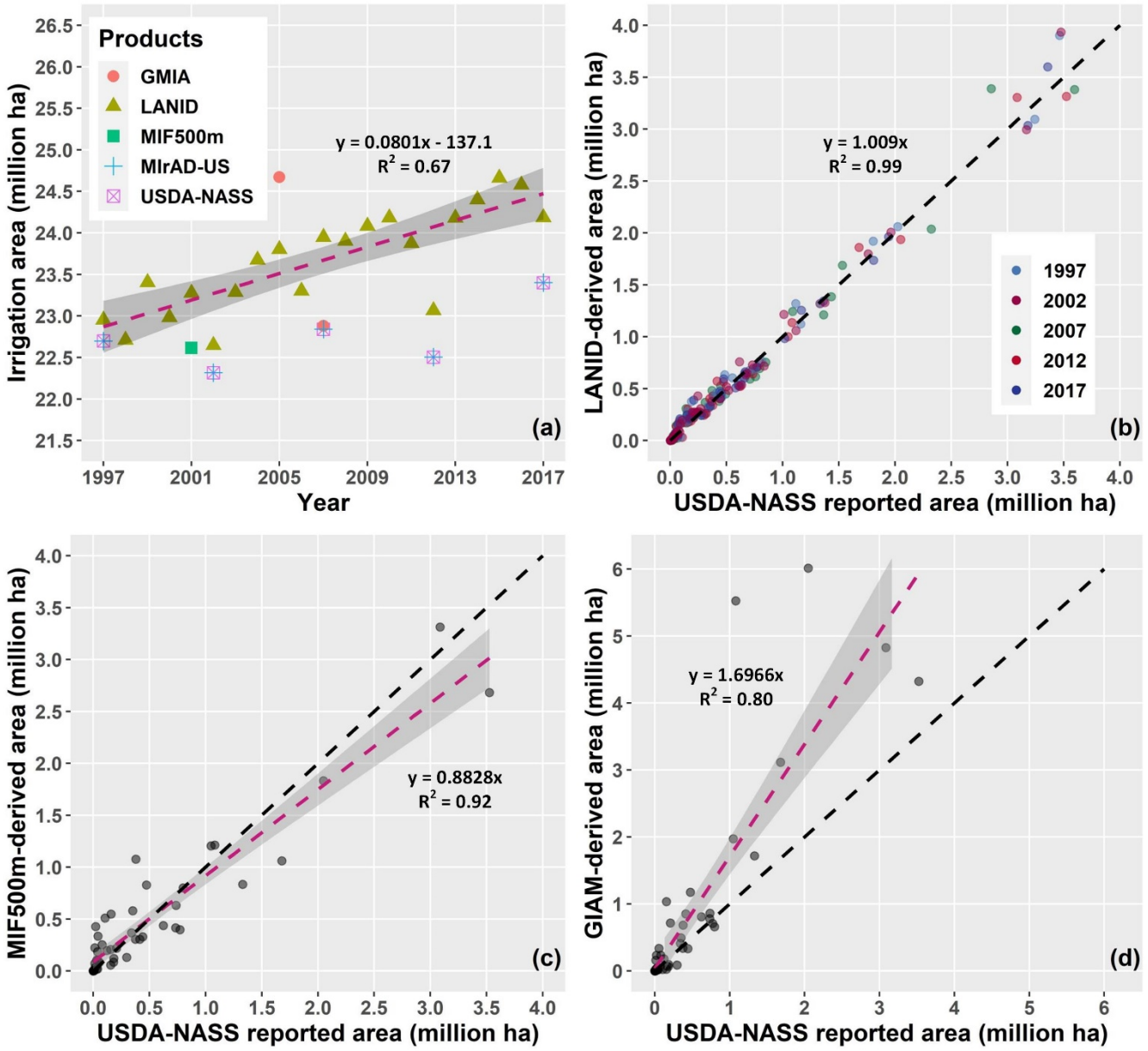

Figure 14: Comparisons of irrigated area between products at the nation (a) and state (b-d) level. (a) LANID-derived nationwide irrigation trend (dashed pink line) and irrigated area of other products; (b) USDA-NASS reported vs. LANID-estimated irrigation area for five census years; (c) USDA-NASS reported (2002) vs. MODIS-estimated (2001) irrigated area (adapted from Ozdogan and Gutman (2008)); (d) USDA-NASS reported (2002) vs. GIAM-estimated (2000) irrigated area. Note the GIAM-estimated nationwide irrigated area (39 million ha) is not shown in (a) due to its exceptionally high value. State-level comparisons between USDA-NASS and MIrAD-US and GMIA are not demonstrated because both products used census data as reference.

The results of pixel-based assessment further reveal the advantages of LANID over other nationwide maps (Table 4). We find that the overall accuracy is generally high for the NKOT region (i.e., Nebraska, Kansas, Oklahoma, and Texas) across all nationwide maps except for GIAM, with mean accuracy ranging from 78.9 % (MIF) to over 95 % (the LANID maps). Similarly, all maps show relatively high overall accuracy for the 11 western states, with values ranging from 82.6 % of MIF to 94.2 % of MIrAD. Despite these maps' reasonable accuracy in the west and even Midwest, they incorrectly assign a considerable number of rainfed fields as irrigated possibly due to coarse resolution and their difficulty separating them in some areas such as the Columbia Plateau Aquifer (Fig. 11). For example, GIAM captures many low-density pixels in the west (Fig. 15c); MIF overestimates the locations with irrigation fraction between 0 and 60 % (Fig. 15b); MIrAD maps irrigated pixels with median fraction around 80 % (Fig. 15a).

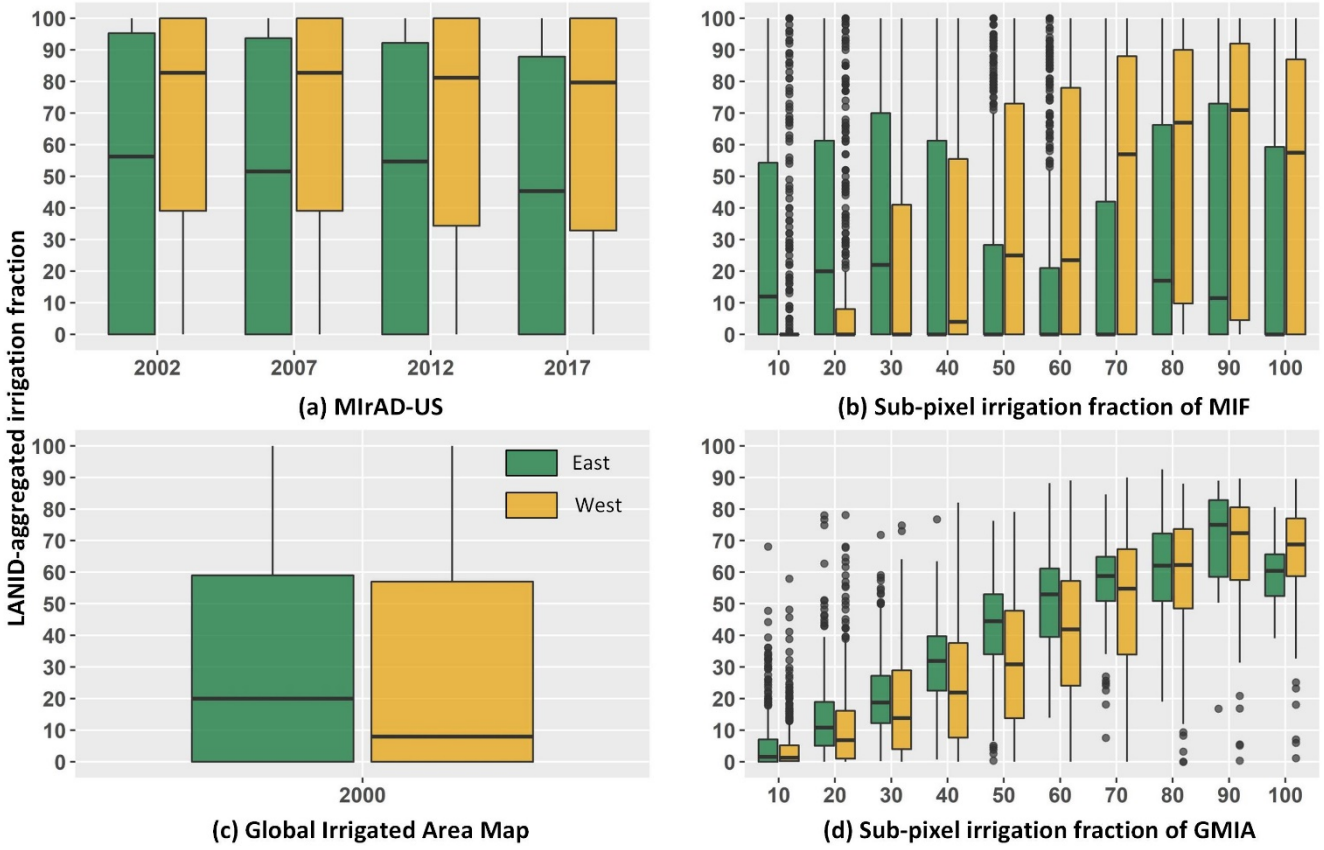

Figure 15: Box plots showing irrigation fraction mapped in each product using LANID as reference. The western and eastern CONUS (separated by red line in Fig. 2) are shown as brown and green, respectively. The 30-m LANID maps were aggregated as irrigation fraction to match the spatial resolution of each product (e.g., 250-m for MIrAD). For binary maps MIrAD and GIAM, five thousand irrigated samples were stratified for both west and east; fifty samples were selected for each irrigation fraction from 1 to 100 % (with increment of 1 %) in MIF and GMIA. The numbers on the horizontal axes of (b) and (d) refer to the maximum value of each bin.

In the eastern U.S., our LANID maps stand out with overall accuracy of 94.4 % – on par with their performance in the western U.S. – whereas other maps show accuracy below 60 %. The extremely low accuracy of MIrAD, MIF, and GIAM in the east is attributable to their missing of most irrigated cropland as well as frequent false identification of rainfed cropland as irrigated (see Fig. 13 as an example), as characterized by omission error rates over 80 % and commission error rates over 45 % for the "irrigated" and "non-irrigated" class, respectively. As a result, MIrAD maps irrigated pixels in the east that have a median irrigated fraction of about 50 % according to LANID (Fig. 15a); GIAM misclassifies a substantial number of low-density pixels (Fig. 15c); MIF substantially overestimates the locations with irrigation fraction beyond 30 % (Fig. 15b).

We also compared our maps to AIM-HPA (i.e., Annual Irrigation Maps – High Plains Aquifer) (Deines et al., 2019), a dataset with the same spatial and temporal resolution as LANID but covering only the High Plains Aquifer. In this region, LANID performs comparably to the HPA-specific dataset, with overall accuracy of 95.9 % vs. 93.2 %, respectively, and Kappa values of 0.89 vs. 0.82.

For a broader 11 western state region, our LANID maps show 92.8 % congruence (Kappa of 0.84) with the reference data from IrrMapper (Ketchum et al., 2020) compared to a 99.1 % (Kappa of 0.98) congruence of the IrrMapper product with its reference data. Such results follow in part from the methods of reference data utilization, as IrrMapper used 60 percent of the validation data used in our comparison for its classifier training. Further differences between LANID and IrrMapper may stem from differences in sampled data and irrigated class definition. For example, the IrrMapper point-based irrigation samples were stratified from verified fields that were digitized in years different from the time of irrigation verification, such that they likely capture permanently irrigated croplands well but may potentially include fields that are partially irrigated or fallowed in any given year. In addition, IrrMapper's reference irrigation samples appear to include both irrigated croplands and other grass-like lands, such as irrigated turfgrass and groundwater- or fluvial-subsidized grasslands and wetlands. This broader and more variable pool of reference data may thus help explain additional observed differences, such as occasionally less distinct field boundaries in IrrMapper as compared with LANID and GI (e.g., lefthand portions of Fig. 11h-k) as well as the slightly higher apparent accuracy of MIrAD (which relies only on vegetation greenness) compared to LANID in the west when assessed against the IrrMapper reference data (Table 4). Thus, while overall performances of LANID and other datasets are similar in overlapping regions like the HPA and the western states, differences in each product's intent and class specificity will likely dictate preferences for specific user applications.

Table 4. Confusion table of pixel-wise accuracy assessment. The overall accuracy, omission error (1 – Producer's accuracy), and commission error (1 – User's accuracy) are in percent. Accuracy values are averaged if multiple-year assessment was conducted. Parenthetical numbers represent the standard deviation.

Maps	Region	Year	Kappa	Overall accuracy	Omission error		Commission error		Sample size	Irrigation sample
					Irrigated	Non-irr	Irrigated	Non-irr		
LANID	West[a]	1997-2017	0.84 (0.07)	92.8 (3.5)	11.4 (6.9)	3.6 (1.0)	6.1 (4.9)	10.7 (8.9)	4433	2284
	NKOT	1997-2017	0.93 (0.02)	96.6 (0.8)	5.9 (1.4)	1.0 (0.2)	1.0 (0.2)	5.6 (1.3)	9994	5002
	East	1997-2017	0.89 (0.01)	94.4 (0.6)	10.7 (1.2)	0.5 (0.1)	0.6 (0.1)	9.7 (1.0)	10000	5000
	HPA[b]	1997-2017	0.89 (0.03)	95.9 (1.1)	4.7 (1.4)	2.3 (0.6)	0.7 (0.2)	13.0 (3.3)	5890	4479

MIrAD	West[a]	2002, 2007	0.84 (0.02)	94.2 (0.8)	10.3 (2.4)	4.3 (0.9)	11.2 (5.4)	4.3 (2.1)	3102	987
	NKOT	2002, 2007, 2012, 2017	0.76 (0.05)	87.8 (2.5)	18.0 (4.4)	6.3 (0.7)	7.1 (1.0)	16.2 (3.4)	9967	5014
	East	2002, 2007, 2012, 2017	0.16 (0.01)	58.0 (0.7)	82.3 (1.1)	1.7 (0.6)	8.7 (2.9)	45.6 (0.4)	10000	5000
MIF[c]	West[a]	2001	0.49	82.6	47.8	7.4	29.9	14.6	3002	747
	NKOT	2001	0.58	78.9	27.2	14.9	17.0	24.3	9985	5001
	East	2001	0.12	55.9	83.6	4.6	21.9	46.7	10000	5000
GIAM	West[a]	2000	0.72	87.6	23.5	6.2	12.6	12.3	3436	1234
	NKOT	2000	0.25	62.6	57.2	17.5	29.0	41.0	10040	5023
	East[a]	2000	0.04	52.2	93.5	2.0	23.6	48.8	10000	5000
AIM-HPA	HPA[b]	1997-2017	0.82 (0.04)	93.2 (1.8)	6.9 (2.4)	6.4 (3.4)	2.1 (1.1)	18.6 (4.8)	5890	4479
	HPA[d]	1997-2017	-	92.7 (1.5)	14.0 (4.5)	3.1 (1.7)	8.5 (2.1)	8.5 (2.1)	1316	519
IrrMapper	West[a]	1997-2017	0.98 (0.01)	99.1 (0.3)	0.3 (0.2)	1.4 (0.3)	2.4 (1.9)	0.3 (0.2)	4433	2284
LANID2012	NKOT	2012	0.84	92.0	10.1	5.8	6.0	9.8	9938	5002
	East	2012	0.49	74.4	49.4	1.9	3.7	33.5	10000	5000

[a] Validation samples from Ketchum et al. (2020). Test samples for the years 1999, 2004, 2005, 2012, 2015, and 2017 were not used because of limited irrigated samples. [b] Validation samples from this study. [c] Irrigated pixels were set as fraction greater than 20 %. [d] Accuracy assessment reported by Deines et al. (2019). NKOT: Nebraska, Kansas, Oklahoma, and Texas.

5 Discussion

5.1 Uncertainty, limitations, and future improvements

Both qualitative and quantitative assessments show extensive improvements of LANID compared to other currently available nationwide maps in terms of spatial detail and temporal frequency. Despite the advances, caution is still needed especially when applying the dataset at the scale of individual fields in the eastern U.S. For example, mapping accuracy in the MAP region is uncertain due to the absence of reference data and the difficulty of collecting aerial ground truth in the area. In addition, map accuracy in the humid East is slightly lower than in the arid and semi-arid West. The quality of maps might also vary over time due to availability of clear Landsat observations. For instance, fewer Landsat images in 2012 constrained map quality and scan-off effects of the ETM+ sensor might remain in some areas.

We took several post-classification steps to improve mapping accuracy, which also introduces limitations to LANID. First, our minimum mapping unit of 5 acres (i.e., 23 Landsat pixels) improved mapping confidence but also excluded smaller irrigated fields, such as fragmented irrigated vegetable fields often found in suburban and peri-urban areas. Second, the assumption that fields equipped with irrigation systems tend to be cropped and irrigated frequently could have incorrectly masked out some irrigated fields historically under long-term and frequent fallow (e.g., irrigated – long-term fallow – irrigated). Lastly, our current version of LANID covers only the period of 1997 to 2017, which might be problematic for users who want

maps outside the study period. However, we hope to regularly update the existing dataset in the future to include the most recent years of available imagery, and, if able, extend the time series back in time through the duration of the Landsat record. Given these uncertainties and limitations, future generations of LANID could benefit from the following improvements. First, we anticipate using our temporally extendable methodology to routinely update LANID, such that coverage could extend prior to 1997 and up to the most recent year. Efforts could also be made to enhance spatial detail (e.g., 10 m resolution) and mapping accuracy, particularly in the humid eastern U.S. where contrasts between irrigated and rainfed crop are obscure. This is practical for recent years when both the revisit frequency and spatial resolution of satellite observations are greatly improved. Lastly, implementation of an irrigation-specific change detection algorithm could help improve the identification and consistency of monitoring variations in irrigation over time.

5.2. Potential applications

Our annual 30-m resolution nationwide LANID maps may be valuable to local, state, and regional water governance bodies, agribusinesses, and the research community for a variety of applications including water use estimation, risk assessment, use as model input, and more.

Our LANID maps could benefit water and agricultural managers by providing insights into irrigation changes (e.g., expansion and abandonment) at geographic and temporal scales relevant to decision-making. Our field-scale, wall-to-wall data will enable local and regional water management organizations, which may not otherwise have sufficient data or resources, to make better decisions that influence regional water availability. For example, state-level water managers and engineers who need to plan how much water to allocate for agriculture could utilize our irrigation distribution and change information to estimate demand. Policy makers may also use LANID to navigate future decision making and to evaluate federal agricultural, bioenergy, and conservation policies (Mccarthy et al., 2020; Lark, 2020).

Our dataset may also be useful for agribusinesses and entities across agricultural supply chains. For example, our maps could be used by companies that seek to reduce risk from water scarcity within their supply chains or lower the water footprint of their sourced products (Brauman et al., 2020). Additional applications may include business decision-making and financial investment (Turral et al., 2010), precise field-level water use estimation and solutions (Sadler et al. 2005), and crop yield prediction and its water resilience (Troy et al., 2015).

A key informant and collaborator in the development of our LANID maps has been the USGS, and the produced outputs may help support several ongoing USGS efforts, such as the National Water Census's efforts to provide water budgets at the watershed level (USGS, 2020c), the National Water-Use Information Program (NWUIP) dissemination of water use data (USGS, 2020a), and the Water Availability and Use Science Program (WAUSP) assessments of regional groundwater availability (USGS, 2020b). The research community within USGS also has high priority goals to improve quantification of crop consumptive water use and project future water use. Our improved estimates of irrigation location, extent, and dynamics could help refine evapotranspiration estimates of irrigated croplands, thereby improving estimates of agricultural water use

from field to aquifer scale and further supporting the ongoing expansion of detailed water use estimates across the continental U.S. (Senay et al., 2016; Senay et al., 2017).

We also hope that our dataset will serve several needs in the broader research community, especially for those who study hydrology, agriculture, and the environment from local to nationwide scales. For example, our 30-m resolution irrigation data could be used to potentially improve the classification accuracy of or add irrigation status to existing USGS and USDA landcover maps (Brown et al., 2020; Lark et al., 2021; Wickham et al., 2021), investigate the relationships among irrigation changes and cropland expansion and abandonment (Lark et al., 2020; Yin et al., 2020), or explore the competition and biophysical interactions between irrigated agriculture and urban expansion (Xie et al., 2019a; Van Vliet, 2019; Bren D'amour et al., 2017). Users of previous coarser resolution irrigation datasets will also benefit from the improvements in spatial detail, product frequency, and map accuracy. Existing nationwide irrigation datasets like MIrAD have been accessed by hundreds of users in academia and government via the USGS EROS website (Brown and Pervez, 2014). These data have been incorporated into studies to evaluate trends in ground and surface water quality, model evapotranspiration and energy-water exchange at the surface boundary layer, and reveal locations at risk of unsustainable irrigation (Brown and Pervez, 2014; Pryor et al., 2016; Seyoum and Milewski, 2016; Jin et al., 2011; Zaussinger et al., 2019). Our 30-m data products will enhance similar types of applications and enable many others through the improved spatial and temporal resolution. To this extent, several organizations have begun using our previously published LANID 2012 for further research and development activities, despite there being only 1 of the presently described 21 annual years of data available; such applications should be further enabled by the current full suite of products and time periods.

Lastly, our collected samples could help generate new threads of irrigation maps for the eastern U.S. Because insufficient ground reference data has long been a bottleneck to producing accurate classifiers for irrigation mapping, our verified locations could facilitate the development and evaluation of new models for irrigation detection, especially when other constraints are becoming relieved due to increasingly available high- to moderate-resolution remote sensing images, development of machine learning algorithms, and open access of cloud computing platforms.

6. Data availability

Our annual LANID maps, their byproducts (i.e., maximum irrigation extent, irrigation frequency, and per-pixel irrigation trends), ~10,000 manually collected ground reference data, and metadata can be accessed via https://doi.org/10.5281/zenodo.5548555 (Xie and Lark, 2021a). All maps are projected to the "Albers Conical Equal Area" projection at 30-m resolution except for the map of irrigation trends of 6-km.

7 Conclusions

This paper presents the only annual, nationwide fine-resolution maps of irrigation extent for the U.S., which are available for each year 1997-2017 and offer several improvements over other products. The increased resolution of the described LANID dataset sets a new standard in spatial detail at the CONUS extent, while the increased mapping frequency and multidecadal coverage enable characterization of irrigation dynamics. Our accuracy assessment shows that the LANID maps provide the most realistic depiction of irrigation extent across the country, with performance that matches or exceeds existing regional datasets.

Moving forward, the LANID maps provide a foundation for refined representations of irrigation distribution and dynamics across the U.S. It is clear from recent research efforts that high quality, frequently updated data on fine-scale irrigation extent is immensely valuable for both the research and application user communities. With these needs in mind, our future intents and interests surrounding LANID may focus on: (1) routinely updating annual maps after 2017; (2) providing finer resolution maps of irrigation extent (e.g., 10m) by fusing multi-source imagery; and (3) improving mapping accuracy in the eastern CONUS.

Appendices

Table A1. The LANID-derived state-level irrigated area (in hectares) of each year between 1997 and 2017 (1997-2008).

States	1997	1998	1999	2000	2001	2002	2003	2004	2005	2006	2007
Alabama	34535	39125	44618	37601	45173	42095	43512	48210	49533	56837	55946
Arizona	379287	355684	352011	354327	353060	337113	351052	348990	349530	342038	326403
Arkansas	1687799	1839858	1886084	1855790	1920171	1859224	1903682	1902655	1886089	1866404	1919269
California	3380488	3151686	3149145	3156261	3184521	3314552	3187264	3172349	3206905	3197729	3094285
Colorado	1210321	1121823	1127185	1114290	1108564	1000578	1102934	1105161	1100720	1070917	1121951
Connecticut	302	807	807	829	910	970	851	801	1251	1108	1013
Delaware	47054	49638	49591	53128	52042	49221	53965	54924	57305	56429	48586
Florida	615570	547328	569116	568295	574083	640918	578654	578092	578447	574716	561719
Georgia	366690	384742	434499	404428	428114	403744	416991	442892	448528	418726	457852
Idaho	1385130	1352224	1339614	1336683	1311422	1319562	1323663	1340630	1340766	1339902	1319951
Illinois	306516	295264	308291	318324	309793	302484	312484	322255	343074	372371	374335
Indiana	168572	170884	170226	180406	169450	173272	212469	211910	211605	224793	221168
Iowa	141592	146916	142392	129494	131310	134782	136684	158873	146813	140562	153320
Kansas	1243244	1321112	1329850	1282021	1283028	1135702	1353488	1288916	1350727	1227553	1318920
Kentucky	13104	13479	12991	12209	13955	13346	17538	19164	21688	25816	23551
Louisiana	415211	451161	458231	442128	488285	428395	453754	432163	445974	438908	421933
Maine	3644	4142	4983	4910	5629	4403	5167	5738	5731	7701	9487
Maryland	46450	47965	44192	48584	53744	47490	50384	56148	56940	56354	50152

Massachusetts	4756	4250	5274	5216	5069	5258	5044	5629	5670	5920	4709
Michigan	179126	174745	186417	202131	189431	189615	204443	210328	233991	256992	229009
Minnesota	219513	223631	236929	233381	219645	236085	230768	240468	232043	225834	227401
Mississippi	526481	529629	641770	570773	627065	567028	599802	568687	603644	517243	604432
Missouri	480854	523644	559171	558573	600994	571590	605685	600251	610383	646444	632748
Montana	754784	716614	730501	728447	753781	750609	734975	756981	743386	747750	764726
Nebraska	3388881	3607761	3737425	3602001	3655262	3303885	3577851	3763770	3713858	3628089	3902377
Nevada	255173	248903	249718	252576	252090	243633	255082	257084	255298	253798	243299
New Hampshire	625	661	934	930	918	891	991	1065	1123	976	782
New Jersey	25712	27451	28717	32253	30855	33095	31175	34197	33369	35184	30257
New Mexico	323098	296609	314995	297562	310916	312938	304907	317588	313720	305273	324526
New York	12503	14324	15970	18173	16761	18620	19341	20163	20029	21209	21336
North Carolina	22569	22641	25847	26482	26672	30930	29181	27337	30732	35506	31644
North Dakota	164616	179741	190039	192953	174264	185754	180438	201479	203502	186949	199093
Ohio	6345	6091	6492	10584	9362	6949	7985	12980	13365	10487	11161
Oklahoma	221859	230949	237608	240967	236309	218499	263921	260352	263092	236626	257870
Oregon	693065	657674	674871	675721	678911	705284	681086	691636	672903	683382	686578
Pennsylvania	2877	2648	2918	4303	4295	4006	4970	5664	5006	6213	5665
Rhode Island	721	755	790	921	903	791	965	944	965	958	1039
South Carolina	39571	38942	44011	45249	46390	45040	50078	53012	57992	61285	58224
South Dakota	245846	251604	260802	241994	256887	227293	242316	257936	269721	250017	279162
Tennessee	12096	18410	20843	21540	24923	25049	30954	26660	34988	37998	42068
Texas	2037060	1832083	1970036	1886396	1902613	1935970	1894429	2020246	2042627	1883622	2061213
Utah	447520	418494	414730	415852	412975	404106	408105	409668	411897	412424	420019
Vermont	459	675	827	905	1143	918	1219	1048	1090	1508	1047
Virginia	15675	17807	18575	23268	20898	22374	23122	25289	28893	28187	28249
Washington	665353	650243	674586	666842	654969	695216	665695	687093	662436	672477	672925
West Virginia	115	224	165	328	378	373	300	531	312	455	373
Wisconsin	168788	169200	177363	175174	177969	176654	174700	179013	181334	183905	181335
Wyoming	591280	549623	552916	552251	550526	520762	552083	546981	553945	546109	545747
CONUS	22952830	22709864	23405066	22983454	23276428	22647066	23286147	23673951	23802940	23301684	23948855

Table A1. Continued (2009-2017).

States	2008	2009	2010	2011	2012	2013	2014	2015	2016	2017
Alabama	60139	63088	60198	68873	70572	74533	76987	81990	78022	80805
Arizona	347354	345935	348800	347701	332402	345229	342976	347084	342758	374399
Arkansas	1884322	1869713	1862017	1856051	1962000	1895565	1884232	1904854	1915934	2005406
California	3188969	3183257	3210136	3193344	3034074	3150194	3098087	3165015	3171492	2993121

Colorado	1097294	1111432	1099495	1090921	982058	1069911	1090256	1085316	1079062	1058369
Connecticut	1240	1146	946	1011	1167	766	1000	964	930	704
Delaware	53855	58197	58583	57379	58263	63623	65377	66345	62686	59182
Florida	571469	575663	574039	577377	533861	581562	577921	578069	575584	524110
Georgia	454795	449800	443450	423956	456294	436233	440079	447356	427585	482965
Idaho	1332914	1350822	1331055	1342894	1343860	1330616	1328663	1340649	1321842	1328081
Illinois	373296	405632	391193	401018	388723	400631	422017	435894	425569	429765
Indiana	232998	224904	251318	239992	219071	271049	269836	277084	274989	274193
Iowa	165879	172773	171304	176592	152614	162926	171756	168785	181923	158593
Kansas	1298163	1293371	1254278	1219387	1255779	1269960	1271563	1298644	1348197	1213904
Kentucky	24637	24648	27565	26845	23918	34820	35942	40236	37892	37695
Louisiana	457305	464418	461525	454552	474357	466391	480660	453071	456294	520158
Maine	10911	9281	11768	13246	12731	13232	14101	12322	12993	12004
Maryland	53551	64218	57960	57262	56885	65756	63208	64878	63111	62859
Massachusetts	5127	5277	5190	5125	4462	4867	4829	4676	4710	4883
Michigan	255967	249827	271441	280475	270287	298783	312146	319282	304834	307379
Minnesota	246865	248258	259921	265191	265084	261758	276892	284753	289736	268822
Mississippi	581096	592122	586089	574756	661108	607189	623127	586732	607843	727048
Missouri	632621	677098	639719	630628	594163	663467	689456	714821	700031	757763
Montana	755680	751866	765259	749722	709597	767409	752198	749607	734882	717839
Nebraska	3809427	3795113	3812085	3906419	3599322	3788075	3890195	3938095	3916648	3932941
Nevada	254701	253634	257118	254508	242259	255488	260470	263629	258504	261773
New Hampshire	1136	979	998	1051	1052	1033	1086	989	824	841
New Jersey	31874	32858	29627	32556	29711	29231	31729	30367	30056	27307
New Mexico	302674	309613	322031	287084	267775	303436	309672	315822	314231	278521
New York	22813	22985	21997	21375	19613	22087	21278	23348	21348	18062
North Carolina	39903	44633	40770	48174	49348	54476	60055	61742	62867	60946
North Dakota	192548	216921	222074	219590	208126	200636	237311	227049	208587	194485
Ohio	12389	16820	15163	17568	16019	20830	19226	21596	20769	21797
Oklahoma	241465	237963	255306	207626	222411	254679	253346	267197	280375	262775
Oregon	679313	689700	683527	672638	601796	681881	686693	687199	693521	630691
Pennsylvania	7463	5875	5829	5862	5100	5071	4593	4810	4193	3633
Rhode Island	1055	899	873	996	903	931	947	973	907	825
South Carolina	62819	60304	60997	70816	75314	78853	79582	78073	83985	83152
South Dakota	282989	300158	316604	305400	247765	310061	311233	310428	306264	273417
Tennessee	47716	50000	62366	72275	82320	95120	99624	105668	98550	95929
Texas	1947439	1958584	2042729	1806539	1734962	1950095	1931265	1990790	1960109	1797103
Utah	410925	413886	410487	415526	408438	409979	411089	407372	409971	404194
Vermont	1343	1497	1467	1250	1429	1135	1024	1176	953	988

Virginia	29632	30258	26965	30214	28495	31826	31587	32060	31459	30626
Washington	684029	689341	683064	675888	643850	688835	693133	687186	681781	649433
West Virginia	532	521	413	562	291	511	614	462	381	515
Wisconsin	197534	200655	213834	214935	208410	206657	216340	220279	222335	220264
Wyoming	554241	556873	553396	552743	506874	553539	554765	555745	552047	535443
CONUS	23902407	24082816	24182969	23875893	23064913	24180935	24400166	24660482	24579564	24185708

Author contributions

Yanhua Xie: conceptualization, method design, result analysis, original draft writing, and manuscript review editing; Holly Gibbs: manuscript review and editing; Tyler Lark: conceptualization, funding acquisition, and manuscript review and editing. All authors have reviewed and agreed on the published version of the manuscript.

Competing interests

The authors declare that they have no conflict of interest.

Acknowledgement

This research was supported by the United States Geological Survey (Award Number: G19AC00080) and the Great Lakes Bioenergy Research Center, U.S. Department of Energy, Office of Science, Office of Biological and Environmental Research (Award Number: DE-SC0018409). The authors would like to thank members of the USGS Water Budget and Estimation Project for sharing verified irrigation data, feedback and ideas for mapping, and insights regarding data use for water estimation. We also appreciate the comments from anonymous reviewers and editors for their helpful suggestions. Any use of trade, firm, or product names is for descriptive purposes only and does not imply endorsement by the U.S. Government.

References

Brandt, J. T., Caldwell, R. R., Haynes, J. V., Painter, J. A., and Read, A. L.: Verified Irrigated Agricultural Lands for the United States, 2002-17, U.S. Geological Survey data release, 2021.

Brauman, K. A., Goodkind, A. L., Kim, T., Pelton, R. E. O., Schmitt, J., and Smith, T. M.: Unique water scarcity footprints and water risks in US meat and ethanol supply chains identified via subnational commodity flows, Environmental Research Letters, 15, 105018, 10.1088/1748-9326/ab9a6a, 2020.

Bren d'Amour, C., Reitsma, F., Baiocchi, G., Barthel, S., Guneralp, B., Erb, K. H., Haberl, H., Creutzig, F., and Seto, K. C.: Future urban land expansion and implications for global croplands, Proc Natl Acad Sci U S A, 114, 8939-8944, 10.1073/pnas.1606036114, 2017.

Brown, J. F. and Pervez, M. S.: Merging remote sensing data and national agricultural statistics to model change in irrigated agriculture, Agricultural Systems, 127, 28-40, 10.1016/j.agsy.2014.01.004, 2014.

Brown, J. F., Tollerud, H. J., Barber, C. P., Zhou, Q., Dwyer, J. L., Vogelmann, J. E., Loveland, T. R., Woodcock, C. E., Stehman, S. V., Zhu, Z., Pengra, B. W., Smith, K., Horton, J. A., Xian, G., Auch, R. F., Sohl, T. L., Sayler, K. L., Gallant, A. L., Zelenak, D., Reker, R. R., and Rover, J.: Lessons learned implementing an operational continuous United States national land change monitoring capability: The Land Change Monitoring, Assessment, and Projection (LCMAP) approach, Remote Sensing of Environment, 238, 111356, 10.1016/j.rse.2019.111356, 2020.

Cui, X., Kavvada, O., Huntington, T., and Scown, C. D.: Strategies for near-term scale-up of cellulosic biofuel production using sorghum and crop residues in the US, Environmental Research Letters, 13, 124002, 2018.

Deines, J. M., Kendall, A. D., and Hyndman, D. W.: Annual Irrigation Dynamics in the U.S. Northern High Plains Derived from Landsat Satellite Data, Geophysical Research Letters, 44, 9350-9360, 10.1002/2017gl074071, 2017.

Deines, J. M., Kendall, A. D., Crowley, M. A., Rapp, J., Cardille, J. A., and Hyndman, D. W.: Mapping three decades of annual irrigation across the US High Plains Aquifer using Landsat and Google Earth Engine, Remote Sensing of Environment, 233, 111400, 2019.

Deines, J. M., Schipanski, M. E., Golden, B., Zipper, S. C., Nozari, S., Rottler, C., Guerrero, B., and Sharda, V.: Transitions from irrigated to dryland agriculture in the Ogallala Aquifer: Land use suitability and regional economic impacts, Agricultural Water Management, 233, 106061, 10.1016/j.agwat.2020.106061, 2020.

Dieter, C. A., Maupin, M. A., Caldwell, R. R., Harris, M. A., Ivahnenko, T. I., Lovelace, J. K., Barber, N. L., and Linsey, K. S.: Estimated use of water in the United States in 2015, US Geological Survey141134233X, 2018.

Enciso, J., Jifon, J., Ribera, L., Zapata, S., and Ganjegunte, G.: Yield, water use efficiency and economic analysis of energy sorghum in South Texas, Biomass and Bioenergy, 81, 339-344, 2015.

ESA: Climate Change Initiative Land Cover http://maps.elie.ucl.ac.be/CCI/viewer/index.php, 2015.

Gong, P., Li, X., Wang, J., Bai, Y., Chen, B., Hu, T., Liu, X., Xu, B., Yang, J., Zhang, W., and Zhou, Y.: Annual maps of global artificial impervious area (GAIA) between 1985 and 2018, Remote Sensing of Environment, 236, 111510, 10.1016/j.rse.2019.111510, 2020.

Hansen, M. C., Potapov, P. V., Moore, R., Hancher, M., Turubanova, S., Tyukavina, A., Thau, D., Stehman, S., Goetz, S., and Loveland, T. R.: High-resolution global maps of 21st-century forest cover change, science, 342, 850-853, 2013.

Jin, Y., Randerson, J. T., and Goulden, M. L.: Continental-scale net radiation and evapotranspiration estimated using MODIS satellite observations, Remote Sensing of Environment, 115, 2302-2319, 2011.

Ketchum, D., Jencso, K., Maneta, M. P., Melton, F., Jones, M. O., and Huntington, J.: IrrMapper: A Machine Learning Approach for High Resolution Mapping of Irrigated Agriculture Across the Western U.S, Remote Sensing, 12, 2328, 10.3390/rs12142328, 2020.

Lark, T. J.: Protecting our prairies: Research and policy actions for conserving America's grasslands, Land Use Policy, 97, 104727, 10.1016/j.landusepol.2020.104727, 2020.

Lark, T. J., Meghan Salmon, J., and Gibbs, H. K.: Cropland expansion outpaces agricultural and biofuel policies in the United States, Environmental Research Letters, 10, 044003, 10.1088/1748-9326/10/4/044003, 2015.

Lark, T. J., Schelly, I. H., and Gibbs, H. K.: Accuracy, Bias, and Improvements in Mapping Crops and Cropland across the United States Using the USDA Cropland Data Layer, Remote Sensing, 13, 968, 10.3390/rs13050968, 2021.

Lark, T. J., Spawn, S. A., Bougie, M., and Gibbs, H. K.: Cropland expansion in the United States produces marginal yields at high costs to wildlife, Nat Commun, 11, 4295, 10.1038/s41467-020-18045-z, 2020.

Loveland, T. R., Reed, B. C., Brown, J. F., Ohlen, D. O., Zhu, Z., Yang, L., and Merchant, J. W.: Development of a global land cover characteristics database and IGBP DISCover from 1 km AVHRR data, International Journal of Remote Sensing, 21, 1303-1330, 2000.

McCarthy, B., Anex, R., Wang, Y., Kendall, A. D., Anctil, A., Haacker, E. M. K., and Hyndman, D. W.: Trends in Water Use, Energy Consumption, and Carbon Emissions from Irrigation: Role of Shifting Technologies and Energy Sources, Environ Sci Technol, 10.1021/acs.est.0c02897, 2020.

McDonald, R. I., Green, P., Balk, D., Fekete, B. M., Revenga, C., Todd, M., and Montgomery, M.: Urban growth, climate change, and freshwater availability, Proceedings of the National Academy of Sciences, 108, 6312-6317, 2011.

Meier, J., Zabel, F., and Mauser, W.: A global approach to estimate irrigated areas – a comparison between different data and statistics, Hydrology and Earth System Sciences, 22, 1119-1133, 10.5194/hess-22-1119-2018, 2018.

Mullet, J., Morishige, D., McCormick, R., Truong, S., Hilley, J., McKinley, B., Anderson, R., Olson, S. N., and Rooney, W.: Energy Sorghum—a genetic model for the design of C4 grass bioenergy crops, Journal of experimental botany, 65, 3479-3489, 2014.

Otkin, J. A., Svoboda, M., Hunt, E. D., Ford, T. W., Anderson, M. C., Hain, C., and Basara, J. B.: Flash Droughts: A Review and Assessment of the Challenges Imposed by Rapid-Onset Droughts in the United States, Bulletin of the American Meteorological Society, 99, 911-919, 10.1175/bams-d-17-0149.1, 2018.

Ozdogan, M. and Gutman, G.: A new methodology to map irrigated areas using multi-temporal MODIS and ancillary data: An application example in the continental US, Remote Sensing of Environment, 112, 3520-3537, 10.1016/j.rse.2008.04.010, 2008.

Ozdogan, M., Rodell, M., Beaudoing, H. K., and Toll, D. L.: Simulating the Effects of Irrigation over the United States in a Land Surface Model Based on Satellite-Derived Agricultural Data, Journal of Hydrometeorology, 11, 171-184, 10.1175/2009jhm1116.1, 2010.

Pekel, J. F., Cottam, A., Gorelick, N., and Belward, A. S.: High-resolution mapping of global surface water and its long-term changes, Nature, 540, 418-422, 10.1038/nature20584, 2016.

Pervez, M. S. and Brown, J. F.: Mapping Irrigated Lands at 250-m Scale by Merging MODIS Data and National Agricultural Statistics, Remote Sensing, 2, 2388-2412, 10.3390/rs2102388, 2010.

Pryor, S., Sullivan, R., and Wright, T.: Quantifying the roles of changing albedo, emissivity, and energy partitioning in the impact of irrigation on atmospheric heat content, Journal of Applied Meteorology and Climatology, 55, 1699-1706, 2016.

Robertson, G. P., Hamilton, S. K., Barham, B. L., Dale, B. E., Izaurralde, R. C., Jackson, R. D., Landis, D. A., Swinton, S. M., Thelen, K. D., and Tiedje, J. M.: Cellulosic biofuel contributions to a sustainable energy future: Choices and outcomes, Science, 356, 10.1126/science.aal2324, 2017.

Rosegrant, M. W., Ringler, C., and Zhu, T.: Water for Agriculture: Maintaining Food Security under Growing Scarcity, Annual Review of Environment and Resources, 34, 205-222, 10.1146/annurev.environ.030308.090351, 2009.

Salmon, J. M., Friedl, M. A., Frolking, S., Wisser, D., and Douglas, E. M.: Global rain-fed, irrigated, and paddy croplands: A new high resolution map derived from remote sensing, crop inventories and climate data, International Journal of Applied Earth Observation and Geoinformation, 38, 321-334, 10.1016/j.jag.2015.01.014, 2015.

Sanderson, M. A., Jolley, L. W., and Dobrowolski, J. P.: Pastureland and hayland in the USA: Land resources, conservation practices, and ecosystem services, Conservation outcomes from pastureland and hayland practices: Assessment, recommendations, and knowledge gaps. Allen Press, Lawrence, KS, 25-40, 2012.

Seager, R., Ting, M., Li, C., Naik, N., Cook, B., Nakamura, J., and Liu, H.: Projections of declining surface-water availability for the southwestern United States, Nature Climate Change, 3, 482-486, 10.1038/nclimate1787, 2012.

Senay, G. B., Friedrichs, M., Singh, R. K., and Velpuri, N. M.: Evaluating Landsat 8 evapotranspiration for water use mapping in the Colorado River Basin, Remote Sensing of Environment, 185, 171-185, 2016.

Senay, G. B., Schauer, M., Friedrichs, M., Velpuri, N. M., and Singh, R. K.: Satellite-based water use dynamics using historical Landsat data (1984–2014) in the southwestern United States, Remote Sensing of Environment, 202, 98-112, 2017.

Seto, K. C., Guneralp, B., and Hutyra, L. R.: Global forecasts of urban expansion to 2030 and direct impacts on biodiversity and carbon pools, Proc Natl Acad Sci U S A, 109, 16083-16088, 10.1073/pnas.1211658109, 2012.

Seyoum, W. M. and Milewski, A. M.: Monitoring and comparison of terrestrial water storage changes in the northern high plains using GRACE and in-situ based integrated hydrologic model estimates, Advances in Water Resources, 94, 31-44, 2016.

Shrestha, D., Brown, J. F., Benedict, T. D., and Howard, D. M.: Exploring the Regional Dynamics of U.S. Irrigated Agriculture from 2002 to 2017, Land, 10, 394, 10.3390/land10040394, 2021.

Siebert, S., Henrich, V., Frenken, K., and Burke, J.: Global map of irrigation areas version 5, Rheinische Friedrich-Wilhelms-University, Bonn, Germany/Food and Agriculture Organization of the United Nations, Rome, Italy, 2013.

Siebert, S., Döll, P., Hoogeveen, J., Faures, J.-M., Frenken, K., and Feick, S.: Development and validation of the global map of irrigation areas, Hydrology and Earth System Sciences Discussions, 2, 1299-1327, 2005.

Teluguntla, P. G., Thenkabail, P. S., Xiong, J., Gumma, M. K., Giri, C., Milesi, C., Ozdogan, M., Congalton, R., Tilton, J., and Sankey, T. T.: Global Cropland Area Database (GCAD) derived from remote sensing in support of food security in the Twenty-First Century: Current achievements and future possibilities, 2015.

Thenkabail, P. S., Biradar, C. M., Noojipady, P., Dheeravath, V., Li, Y., Velpuri, M., Gumma, M., Gangalakunta, O. R. P., Turral, H., and Cai, X.: Global irrigated area map (GIAM), derived from remote sensing, for the end of the last millennium, International Journal of Remote Sensing, 30, 3679-3733, 2009.

Troy, T. J., Kipgen, C., and Pal, I.: The impact of climate extremes and irrigation on US crop yields, Environmental Research Letters, 10, 054013, 10.1088/1748-9326/10/5/054013, 2015.

Turral, H., Svendsen, M., and Faures, J. M.: Investing in irrigation: Reviewing the past and looking to the future, Agricultural Water Management, 97, 551-560, 2010.

USDA-NASS: 2017 Census of Agriculture, Summary and State Data, Geographic Area Series, Part 51, AC-17-A-51, in, Washington D.C., USA, 2019.

USDA-NASS: https://www.usda.gov/media/blog/2021/02/11/usda-invests-data-agricultural-irrigation-improvements, 2021.

https://www.ers.usda.gov/topics/farm-practices-management/irrigation-water-use/background/, last

USGS: Water Availability and Use Science Program: https://www.usgs.gov/water-resources/water-availability-and-use-science-program, 2020a.

National Water Census: https://www.usgs.gov/mission-areas/water-resources/science/national-water-census-water-use, last

USGS: USGS Water Use Data for the Nation: https://waterdata.usgs.gov/nwis/wu, 2020c.

van Vliet, J.: Direct and indirect loss of natural area from urban expansion, Nature Sustainability, 2, 755-763, 10.1038/s41893-019-0340-0, 2019.

Wardlow, B. D. and Callahan, K.: A multi-scale accuracy assessment of the MODIS irrigated agriculture data-set (MIrAD) for the state of Nebraska, USA, GIScience & remote sensing, 51, 575-592, 2014.

Wickham, J., Stehman, S. V., Sorenson, D. G., Gass, L., and Dewitz, J. A.: Thematic accuracy assessment of the NLCD 2016 land cover for the conterminous United States, Remote Sensing of Environment, 257, 112357, 10.1016/j.rse.2021.112357, 2021.

Xie, Y. and Lark, T. J.: LANID-US: Landsat-based Irrigation Dataset for the United States [dataset], https://doi.org/10.5281/zenodo.5548555, 2021a.

Xie, Y. and Lark, T. J.: Mapping annual irrigation from Landsat imagery and environmental variables across the conterminous United States, remote Sensing of Environment, 260, 1-17, 10.1016/j.rse.2021.112445, 2021b.

Xie, Y., Weng, Q., and Fu, P.: Temporal variations of artificial nighttime lights and their implications for urbanization in the conterminous United States, 2013–2017, Remote Sensing of Environment, 225, 160-174, 10.1016/j.rse.2019.03.008, 2019a.

Xie, Y., Lark, T. J., Brown, J. F., and Gibbs, H. K.: Mapping irrigated cropland extent across the conterminous United States at 30 m resolution using a semi-automatic training approach on Google Earth Engine, ISPRS Journal of Photogrammetry and Remote Sensing, 155, 136-149, 10.1016/j.isprsjprs.2019.07.005, 2019b.

Xu, T., Deines, J., Kendall, A., Basso, B., and Hyndman, D.: Addressing Challenges for Mapping Irrigated Fields in Subhumid Temperate Regions by Integrating Remote Sensing and Hydroclimatic Data, Remote Sensing, 11, 370, 10.3390/rs11030370, 2019.

Yin, H., Brandão, A., Buchner, J., Helmers, D., Iuliano, B. G., Kimambo, N. E., Lewińska, K. E., Razenkova, E., Rizayeva, A., Rogova, N., Spawn, S. A., Xie, Y., and Radeloff, V. C.: Monitoring cropland abandonment with Landsat time series, Remote Sensing of Environment, 246, 111873, 10.1016/j.rse.2020.111873, 2020.

Zaussinger, F., Dorigo, W., Gruber, A., Tarpanelli, A., Filippucci, P., and Brocca, L.: Estimating irrigation water use over the contiguous United States by combining satellite and reanalysis soil moisture data, Hydrology and Earth System Sciences, 23, 897-923, 10.5194/hess-23-897-2019, 2019.